frontiers in Earth Science

ORIGINAL RESEARCH
published: 28 May 2021
doi: 10.3389/feart.2021.586210

Sponge Takeover from End-Permian Mass Extinction to Early Induan Time: Records in Central Iran Microbial Buildups

Aymon Baud[1], Sylvain Richoz[2], Rainer Brandner[3], Leopold Krystyn[4], Katrin Heindel[5], Tayebeh Mohtat[6], Parvin Mohtat-Aghai[3] and Micha Horacek[7]*

[1] Institute of Earth Sciences, Lausanne University, Lausanne, Switzerland, [2] Department of Geology, Lund University, Lund, Sweden, [3] Institute of Geology and Palaeontology, University of Innsbruck, Innsbruck, Austria, [4] Department of Palaeontology, University of Vienna, Vienna, Austria, [5] GeoZentrum Nordbayern, Paleobiology Section, University of Erlangen-Nuñrnberg, Erlangen, Germany, [6] Geological Survey of Iran, Tehran, Iran, [7] Institute of Lithospheric Research, Vienna University, Vienna, Austria

OPEN ACCESS

Edited by:
Spencer G. Lucas, New Mexico Museum of Natural History and Science, United States

Reviewed by:
Zhong-Qiang Chen, China University of Geosciences Wuhan, China
Dieter Korn, Museum of Natural History Berlin (MfN), Germany

***Correspondence:**
Aymon Baud
aymon.baud@unil.ch

Specialty section:
This article was submitted to Paleontology, a section of the journal Frontiers in Earth Science

Received: *22 July 2020*
Accepted: *23 April 2021*
Published: *28 May 2021*

Citation:
Baud A, Richoz S, Brandner R, Krystyn L, Heindel K, Mohtat T, Mohtat-Aghai P and Horacek M (2021) Sponge Takeover from End-Permian Mass Extinction to Early Induan Time: Records in Central Iran Microbial Buildups. Front. Earth Sci. 9:586210. doi: 10.3389/feart.2021.586210

The end-Permian mass extinction was the most severe biotic crisis in Earth's history. In its direct aftermath, microbial communities were abundant on shallow-marine shelves around the Tethys. They colonized the space left vacant after the dramatic decline of skeletal metazoans. The presence of sponges and sponge microbial bioherms has largely gone unnoticed due to the sponges' size and the cryptic method of preservation. In addition to sponge dominated facies recently described in South Armenia and Northwestern Iran, we describe here sponge-microbial bioherms cropping out in two well-known Permian-Triassic boundary localities: the Kuh-e Hambast section, south-east of Abadeh city and the more distal Shahreza section, near Isfahan. In both sections, the extinction horizon is located at the top of an upper Changhsingian ammonoid-rich nodular limestone, called *Paratirolites* limestone. At Kuh-e Hambast, the overlying decimetric thick shale deposit called "boundary clay," the latest Permian in age, is conformably overlain by well-dated transgressive basal Triassic platy limestone containing four successive levels of decimeter to meter scale, elongated to form cup-shaped mounds made of branching columnar stromatolites. Sponge fibers from possibly keratose demosponge, are widely present in the lime mudstone matrix. At the Shahreza section, above the extinction level, the boundary clay is much thicker (3 m), with thin platy limestone intervals, and contains two main levels of decimeter to meter scale mounds of digitate microbialite crossing the Permian-Triassic boundary with similar sponge fibers. Three levels rich in thrombolite domes can be seen in the overlying 20 m platy limestone of earliest Triassic age. Sponge fibers and rare spicules are present in their micritic matrix. These sponge fibers and spicules which are abundant in the latest Permian post-extinction boundary clay, followed microbial buildups during the Griesbachian time.

Keywords: keratose demosponge, carbonate mounds, end-permian mass extinction, metazoan bioherms, Induan

INTRODUCTION

During the end-Permian mass extinction (EPME) and during the repercussion of its aftermath, the carbon cycle experienced large-scale perturbations over the course of millions of years (Atudorei, 1999; Payne et al., 2004; Corsetti et al., 2005; Richoz, 2006; Horacek et al., 2007a,b,c, 2009; Richoz et al., 2010; Korte and Kozur, 2010, amongst others). This period was marked by a major crisis in carbonate systems: the skeletal carbonate factory was replaced by a non-skeletal carbonate factory (Baud et al., 1997, 2002, 2007; Baud, 1998; Kershaw et al., 1999, 2007; Leda et al., 2014; Woods, 2014). Along the southern margin of the Cimmerian terrane (**Figure 1A**), well-developed highly fossiliferous Late Permian giant carbonate platforms can be found. This prolific inter-tropical Late Paleozoic skeletal carbonate factory ceased abruptly and was replaced first by low-carbonate deposit (boundary clay), then by a non-skeletal carbonate factory.

In Central Iran, from Kuh-e Hambast near Abadeh to Shahreza section close to Isfahan (**Figure 1**), "unusual" fabrics of the basal Triassic carbonate sediments were controversially described to date as stromatolites, algal limestone, thrombolite zone or synsedimentary abiotic carbonate cement layers or crusts.

The first detailed description of the earliest Induan limestone of the Abadeh sections was focused on about 1.6 m thick interval of stromatolites and thrombolites within the *Hindeodus parvus* conodont Zone (Taraz et al., 1981). Gallet et al. (2000) confirmed the finding of *H. parvus* at the base of the Abadeh stromatolite unit (Korte et al., 2004a,b) and Kozur (2005, his Figure 3) otherwise, reported their first *H. parvus* at 1.2 m above the top level of the *Paratirolites* limestone and by ignoring Gallet et al. (2000) shifted the Permian-Triassic boundary above their reduced 0.5-m-thick stromatolite unit. Finally, Richoz et al. (2010) illustrated *H. parvus* at the base of the 1.6-m-thick Abadeh branching stromatolite unit thus confirmed the original boundary position as we use here (**Figure 2**).

This earliest Triassic unit has also been referred to as the "Thrombolite zone" (Baghbani, 1993). Working on the same sections, Heydari et al. (2003) and Heydari and Hassanzadeh (2003) claimed to have found shallow water carbonate seafloor precipitates. This was disputed by Zong-jie (2005) who argued for a deeper microbialites. Richoz (2006) and Baud et al. (2007) later confirmed the first view of a microbial buildup succession. However, Leda et al. (2014) while discussing biotic and abiotic processes, without carrying out detailed studies on Abadeh section, aligned with abiotic calcite fan. To resolve the debated research assertions, interpretations and age of these carbonates, we studied extensively the 1.6 m thick carbonate unit above the extinction event in Abadeh area (Kuh-e Hambast C section) and a 20 m thick carbonate unit at Shahreza section. Looking at the macro- and micro-structures from outcrop to thin section scale, we found a great amount of microbial buildups and sponges, some with visible sponge tissue in the lime mud matrix. According to Luo and Reitner (2014) who studied the convergence evolution of microbialite and sponge in the Phanerozoic, this type of calcified spongin tissue possibly belongs to keratose demosponge.

Sponge microbial buildups (SMB) of Abadeh and Shahreza sections were found after fieldwork in 2011 and our new results were presented at the 20th International Sedimentological Congress (Baud, 2018). Comparative study of the Central Iran basal Triassic mounds revealed that they match with the newly published sponge-microbial buildups (SMB) of South Armenia (Sahakyan et al., 2017; Friesenbichler et al., 2018).

GEOLOGICAL SETTING

Between Gondwana and Eurasia, the Cimmerian microcontinent separate two oceans; the newly opened Permo-Triassic Neo-Tethys facing Gondwana and the old Paleo-Tethys to the North (**Figure 1A**).

The Gondwana Margin

Along the Zagros mountain range (S. Iran) from the Gondwana part or southern margin of the Neo-Tethys, stromatolites and thrombolites are present as microbial-metazoan bioherms at the basal Kangan Formation (Baghbani, 1993) and have been recently described in detail (Wei et al., 2005; Insalaco et al., 2006; Wang et al., 2007, 2020; Heindel et al., 2015, 2018; Foster et al., 2019, supplementary materials).

The Cimmerian Margins

Along the northern Cimmerian margin, Paleo-Tethys, stromatolites and thrombolites are widespread in the lower part of the Elika Formation (Induan) of the northern Iran Alborz mountain range (Altiner et al., 1980; Horacek et al., 2007b; Gaetani et al., 2009; Maaleki-Moghadam et al., 2019).

Along the southern Cimmerian margin of Neo-Tethys, new types of sponge-microbial buildups are found in the lower Induan (Baud and Richoz, 2019) limestone of Southern Armenia and of Central Iran (**Figure 1B**). On the southern margin along the Cimmerian block, some localities close to the present-day NW Iran border have a well-developed highly fossiliferous upper Permian succession. In the past, Russian paleontologists created new stage names such as Dzhulfian and Dorashamian in these localities. Between Southern Armenia and Central Iran, we observed the following succession from the latest Permian to the earliest Triassic time:

1- A pre-extinction red ammonoid limestone called *Paratirolites* limestone;

2- A latest Permian post-extinction "boundary clay" (BC), rich in limy clay;

3- A basal Triassic platy limestone (PL) with or without sponge-microbial buildups (SMB).

Kuh-e Hambast C Section, Abadeh Area

The Abadeh area is located in central southern Iran, about 150 km southeast of Isfahan (**Figure 1B**) and the Kuh-e Hambast C section (Coord.: 30°54'53.65"N, 53°13'3.94"E, altitude 2,000 m) is situated 80 km SE of Abadeh town (Taraz, 1969, 1971, 1973, 1974). This author separated the Permian and Triassic parts into well-defined lithostratigraphic units, numbered 1–7 for the Permian part, with Unit 7 consisting of the end-Permian red

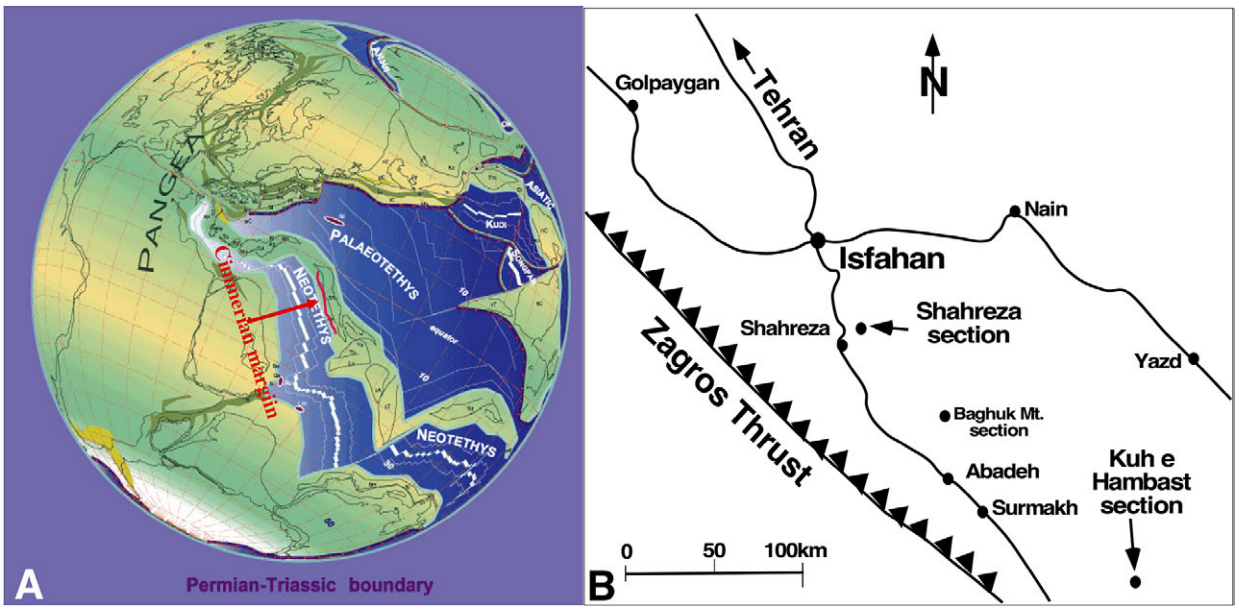

FIGURE 1 | (A) 250 Ma paleogeographic map (Stampfli and Borel, 2002, modified) showing the Cimmerian margin (red line). **(B)** Map of Central Iran showing the main relevant localities and the examined sections.

ammonoid limestone, and sections of the Hambast Formation, with red shale at the top [boundary clay (BC)]. The Lower Triassic section is subdivided into Units A to E, with Unit A composed of the basal Triassic platy limestone (Taraz, 1974). In later publications which focused on Shahreza, the boundary clay (BC) was merged with the Lower Triassic Elika Formation (also called Elikah in Taraz et al., 1981).

A very detailed description of more than five Kuh-e Hambast Permian to Lower Triassic sections have been done by the Iranian Japanese Research Group (Bando, 1981; Taraz et al., 1981). The Abadeh PT transition with bioturbated Lower Triassic succession was later interpreted by Wignall and Twitchett (2002) as a dysaerobic facies.

The magnetostratigraphy of the Permian-Triassic Boundary Interval (PTBI) was studied by Gallet et al. (2000) following the biochronology done by L. Krysyn on conodont and ammonoides composed of Earliest Induan *Hindeodus parvus* conodont Zone at the base of the microbialite interval. A sedimentological description of this interval was published, with the first ever carbon isotope curve highlighted (Heydari et al., 2000, 2001, 2003). This was followed by further detailed carbon isotope studies (Korte et al., 2004a,b; Richoz, 2006; Horacek et al., 2007a; Richoz et al., 2010). Carbon and strontium isotopic chemostratigraphy was the subject of discussion in other papers (Korte et al., 2010; Liu et al., 2013). The $^{87}Sr/^{86}Sr$ seawater curve across the PTBI, which focused on conodonts analysis of Abadeh and South China has been revised (Dudás et al., 2017). These authors estimated a depositional rate of the platy limestone to Kuh-e Hambast at around 16 m/My.

The latest Permian earliest Triassic conodont zonation for Abadeh, which has been a subject of debate, is presented in section "Introduction," illustrated in **Figures 2A,B**, discussed in section "Biochronology." A detailed evaluation of this PTB debate can be found in Horacek et al. (2021). In this study, we used the Lower Triassic biochronology of Richoz et al. (2010).

The Shahreza Section

The Shahreza section (Coordinates: N32°07'18"; E51°57'33", Altitude: 1,820 m) lies 14.5 km NNE of Shahreza town and 3.8 km ESE of Shahzadeh Ali Akbar village, which is about 180 km NW of Abadeh (**Figure 1**). The Triassic section of the locality is generally more shaly compared to Abadeh, and it is situated in a more distal and deeper environmental setting (Richoz et al., 2010).

The first mention of the section was during the presentation of its upper Permian magnetostratigraphy, which was demonstrated without a lithology scheme (Besse et al., 1998). A short description with well-illustrated figures showing some basal Triassic microbialite mounds was done by Heydari et al. (2000), this was followed by a carbon isotope study (Heydari et al., 2001). A detailed description of sections with localization of some microbialite levels was later documented (Mohtat-Aghai and Vachard, 2003, 2005, Kozur, 2007). A Changhsingian conodont zonation extending to the early Induan was presented by Kozur (2004). Baud et al. (2007) gave a short account of two microbialite levels that aligned with the SMB2 and SMB3 of this study (**Figures 3A–C**). A further carbon isotope curve based on Kozur's zonation and lithology was presented by Korte et al. (2004b).

This was followed by new detailed carbon isotope curves and fine lithological surveys (Richoz, 2006; Heydari et al., 2008; Richoz et al., 2010; Shen et al., 2013). These studies all had results that were in consonance. Based on the feature of the PTBI at the Shahreza section and Sr content, Heydari et al. (2012, 2013)

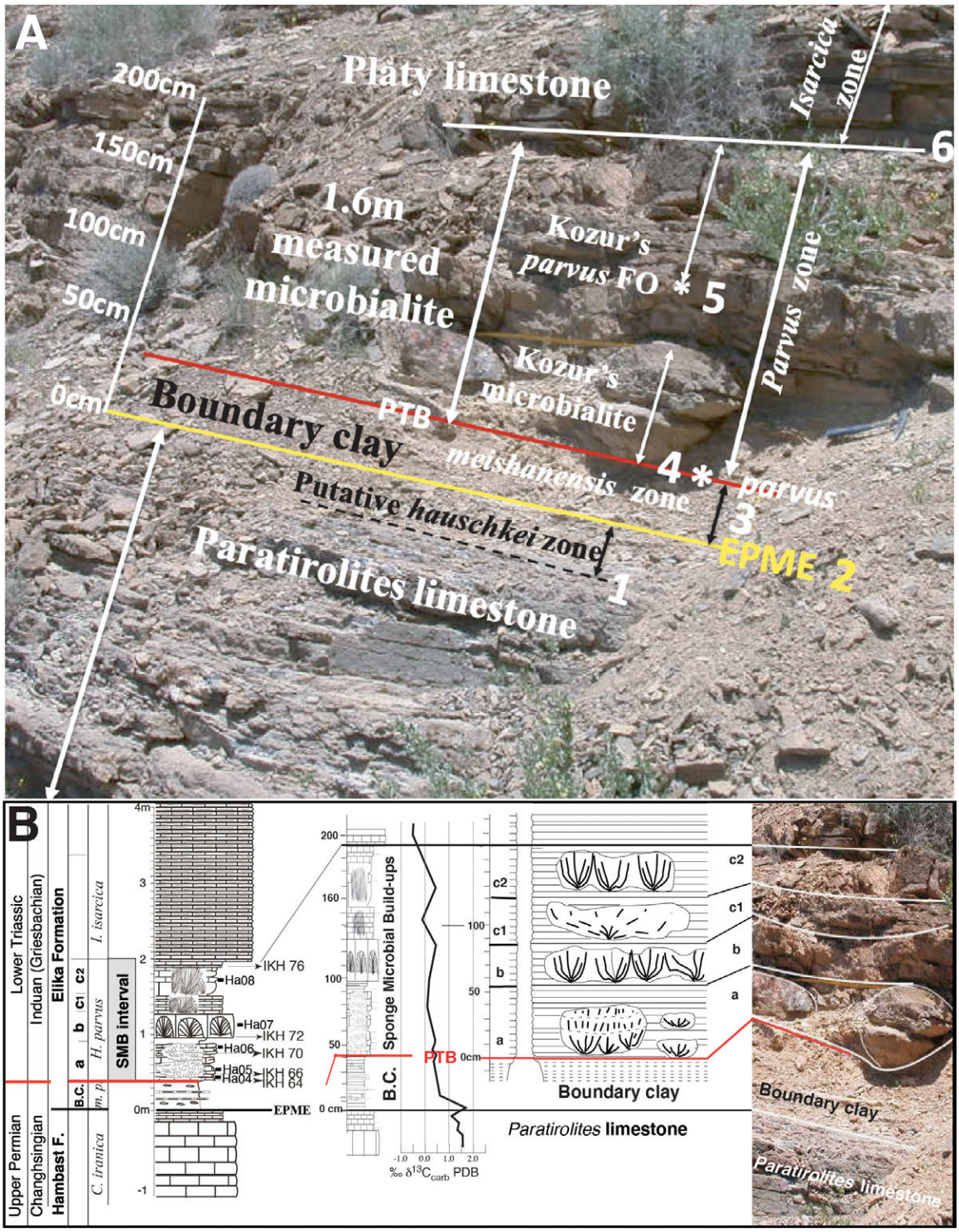

FIGURE 2 | The Permian-Triassic transition at the Kuh-e Hambast C section. **(A)** Field view with 1- base of the pre-extinction *C. hauschkei* zone near the top of the *Paratirolites* limestone; 2- EPME level at the top of the *Paratirolites* limestone; 3- the 30 cm-thick boundary clay with the *H. meishanensis–praeparvus* conodont Zone; 4- *H. parvus* FO (4*) according to Taraz et al. (1981), Gallet et al. (2000), and Richoz et al. (2010) with the adopted Permian-Triassic boundary (PTB), and base of the *H. parvus* zone; 5- Kozur's *H. parvus* FO finding (*5), 120 cm above EPME, Kozur's PTB and base Kozur's *H. parvus* zone; (Korte et al., 2004a) 6- base of the *I. isarciaca* zone. **(B)** Detailed lithology and a $\delta^{13}C_{carb}$ isotope curve (Richoz, 2006) and the SMB levels, numbered a to c2. In the middle, sketch of the bowl or pancake-like structure showing the radiating texture of the microbial laminated columns, typical of digitate stromatolite. On the right-hand side is part of the above **(A)** fieldview. Caption: thick horizontal red line = Permian-Triassic boundary, C., *Clarkina*; H., *Hindeodus*; I., *Isarcicella*; B.C., boundary clay; F., Formation; m-p, *meishanensis–praeparvus* conodont Zone; a, b, c1, and c2 represents the SMB levels explained in the text. EPME, End of Permian Mass Extinction horizon.

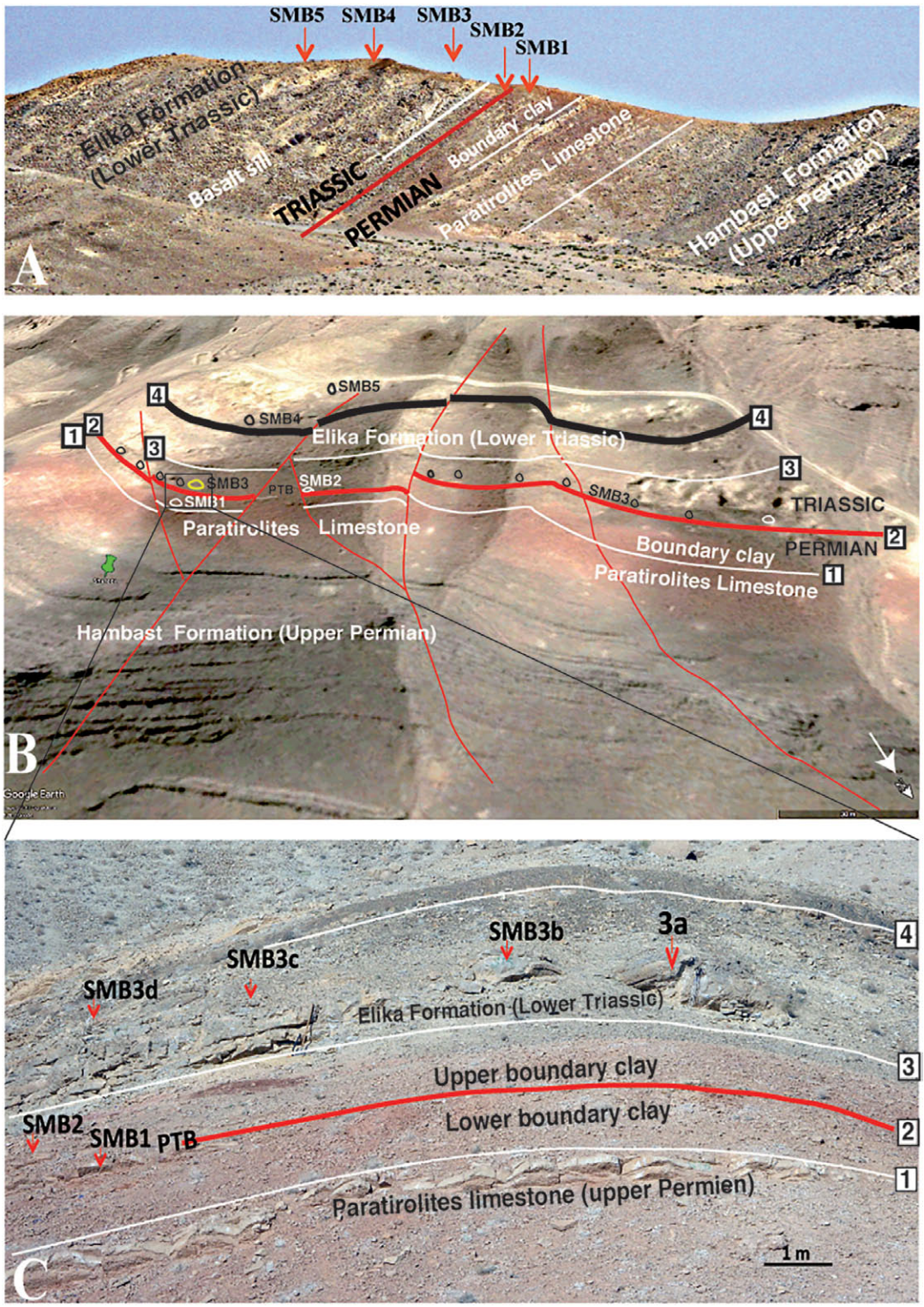

FIGURE 3 | The Shahreza section, profile and upper views. **(A)** View from the SE with the position of the five SMB horizons starting from the post extinction latest Permian (SMB1) and extending to the lower Dienerian (SMB5). Red line, PTB; white line–lithological boundary. **(B)** Google Earth view of the Shahreza section; upper part of photo shows white dirt road to Shahreza (toward the left), white arrow to the north and a 30 m black scale in the lower right corner. 1: EPME -extinction horizon on the *Paratirolites* limestone, base of the Elika Formation. 2: PTB, Permian-Triassic boundary (thick red line). 3: Base of the platy limestone, Elika Formation. 4: Basalt sill, SMB1 to 5 are the sponge-microbial levels. The Heydari 3a is the section with yellow color. Thin red lines show faults. **(C)** Panoramic view of the rectangle in **(B)** with the Permian-Triassic transition levels. Scale bar = 1 m. Numbers 1–4: same as in **(B)**. SMB1 and SMB2 belong to the lower sponge-microbial levels.

presented a new hypothesis on aragonite and calcite sea changes, as well as a new corrected carbon isotope curve based on Sr content, and in accordance with putative primary mineralogy (aragonite and calcite).

In comparison with the microbialites from Abadeh, which are restricted to the earliest Induan *Hindeodus parvus* conodont Zone, the Shahreza carbonate mounds are distributed over a longer period of time and consist of at least five sponge microbialite buildup horizons (SMB1 to SMB5, **Figures 3A,B**). Also, calcified sponge tissues and spicules were observed in the lime mud matrix.

It should be noted that the boundary clay unit (BC) have a greater thickness in Shahreza (about 3 m) than in Abadeh (0.3 m) and is subdivided into 3 parts, a lower BC that is correlated with the Abadeh BC (*H. meishanenesis* conodont Zone), a middle BC with papery limestone and an upper BC with platy limestone (*Hindeodus parvus* conodont Zone).

RESULTS: LITHOLOGY, FACIES, AND MICROFACIES DESCRIPTIONS

The results and illustrations presented below come from fieldwork and microscopic examination of collected samples.

The Kuh-e Hambast C Section of the Abadeh Area

The Permian-Triassic transition in the central Kuh-e Hambast mountain range of the Abadeh area shows a thin post-extinction interval of clayey marls (called boundary clay) capped by a 1.60 m thick layer of successive mounds with numerous arborescent structures.

This layer consists of decimetric buildups distributed within four successive levels (**Figure 2B**, level a, b. c1, and c2), and embedded in thin-bedded platy lime mudstone. They have been seen spread across the whole area, with a corresponding thickness of 1.6 m. The age of the earliest Induan *Hindeodus parvus* conodont Zone at their base is well recorded. The supposed Permian age is discussed and refuted in Horacek et al. (2021) and in section "Biochronology."

The macrofacies consist of a decimeter to meter scale elongated to form a bowl or cup-shaped microbial buildups (**Figures 4A,B**) showing what we call here digitate stromatolite as published in Kershaw et al. (2007, their Figure 13A), or branching stromatolite in Baud et al. (2007, their Figures 3, 4) with clearly finely laminated branched columns producing smaller columns (**Figure 4E**). The term digitate stromatolite is discussed in detail in section "Crystal Fans, Carbonate Crust, Digitate Microbialite, or Digitate Stromatolites?"

As illustrated in the outcrop (**Figure 4**) and thin sections (**Figure 5**), these bioherms are composed of thinly laminated columns protruding from a common leiolitic base or core, and growing side by side as columnar stromatolite. From a distant view, they look like calcium carbonate crystal fans (CCFs) and were regarded as such by Heydari et al. (2003) and by Leda et al. (2014) with some reservations ("enigmatic calcite fan layers"). However, a close examination in the field and under microscope eliminates these doubts.

As shown by **Figures 5A,D,E**, crystals with fine acicular habit and square-tipped terminations, that are typical of early aragonite, grew on the side of the stromatolite columns. These last structures are probably abiotic in origin and should be the only structures referred to as CCFs. The lime mud matrix is usually rich in calcified sponge fibers or spicules (**Figures 5A–C**), which is similar to the sponge spike matrix described by Leda et al. (2014, **Figures 9B–D**). According to Luo and Reitner (2014), these types of spicules belong to putative calcified keratose demosponge tissue. Additionally, rare ostracods are also present. Asymmetric and bent digitate stromatolite branches are possible evidence of the occurrence of currents at the lower section (2 in **Figure 4F**). A unique tempestite deposit with reworking carbonate centimetric clasts has been observed, probably due to the occurrence of a distal storm event (lower b in **Figure 4C**). The growth of the bioherms were temporarily halted by this event but recovered soon after.

A description of the four successive levels a, b, c1, and c2 of the decimetric buildups (**Figures 2**, **4**) is given below:

- Level **a** is about 40-cm-thick and holds bowl-shaped fanning "digitate stromatolite" bioherms up to 35-cm-high and 50 cm in diameter (**Figure 4A**), as well as single pancake-shaped bioherms composed of brush-like systems of branching vertical stromatolite columns, 10–20 cm high and 40 cm to 1 m in elongation (**Figure 4B**).

- Level **b** is characterized by more or less continuous sponge-microbialite distributing an in-stratal interval up to 30 m, with buildups thickness between 20 and 30 cm (**Figures 2D**, **4D,F**). Interestingly, two parts are present in the second level b: the lower one showing reworked clasts (tempestite, **Figure 4C**) and the upper one, which is part of the sponge-microbial bioherm.

-Level **c1** is discontinuous, about 35 cm thick and shows both elongated pancake-shaped bioherms up to 4 m in length of shrubby "stromatolite columns" and cup-shaped bioherms, about 50 cm in diameter (**Figure 4F**).

-The top level **c2** is about 30 cm thick, and also holds pancake-shaped bioherms made of botryoidal fanning "digitate stromatolite" (4 in **Figure 4F**).

The calcium carbonate supersaturated seawater induced a very early diagenetic replacement of the former organic fragments of spongin tissue or sponge spicules within the lime-mudstone around to the sponge-microbial buildups, as shown in the microfacies of **Figure 5**. The surrounding platy limestone consists of a thinly bedded, partly bioturbated micritic lime-mudstone successions (in some parts, it was almost vermicular limestones) and peloidal packstone layers with intercalated marls.

Close to the base of the overlying unit, large oncoids (about 5 cm in diameter) have been found. Similar accumulation of small oncoids have also been reported in sediments of the same age (*Isarcicella isarcica* conodont Zone) from the Zal and Ali Bashi sections of Northwestern Iran (Richoz et al., 2010; Leda et al., 2014). This Griesbachian thin limestone succession (15–17 m) shows a low subsidence rate, which changes drastically during the Dienerian period to an about 500 m thick platy limestone succession (Horacek et al., 2007b).

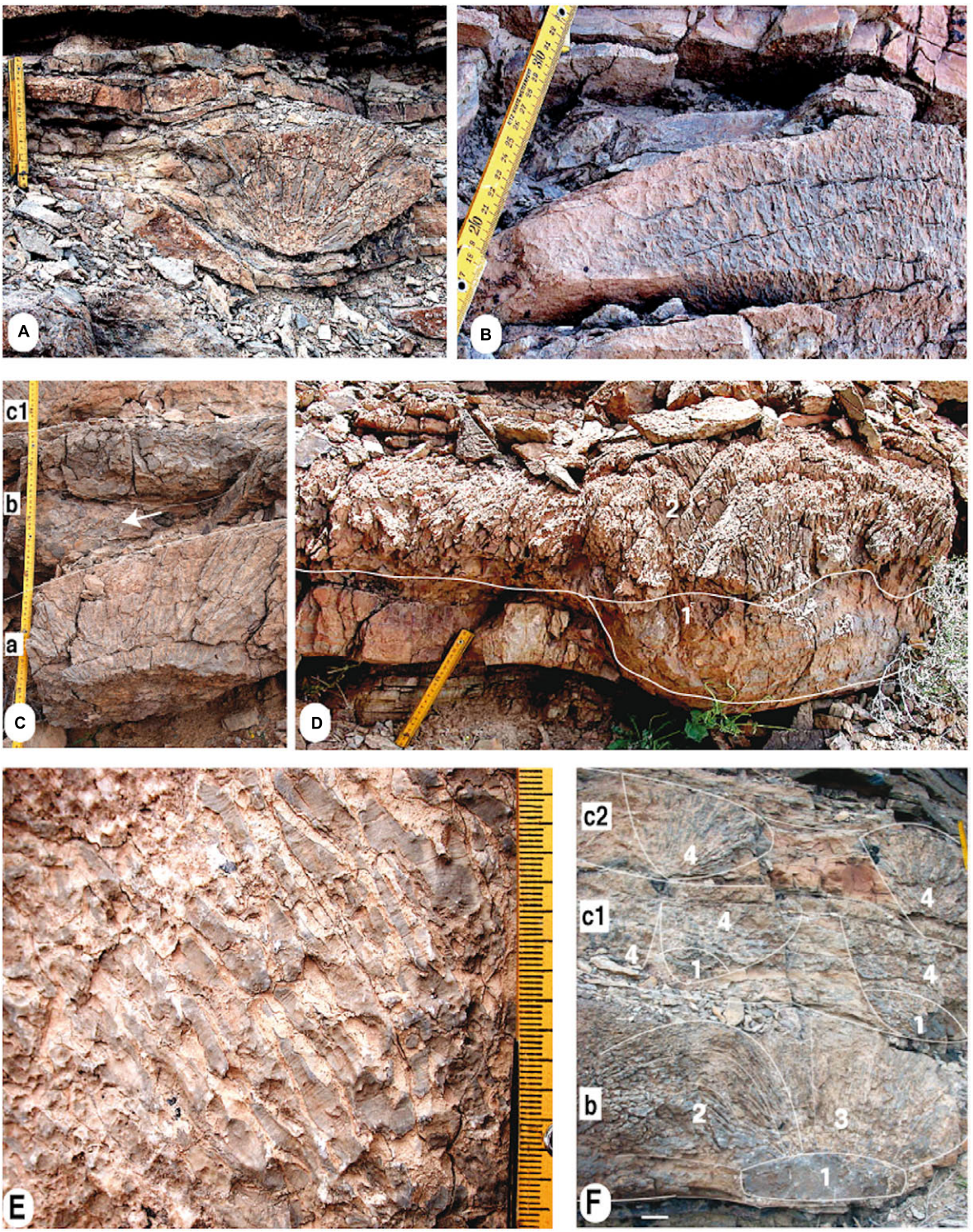

FIGURE 4 | Outcrop views of the SMB levels a, b, c1, and c2 at the Kuh-e Hambast section. **(A)** Bowl-like structure with dark colored fan-shaped branches of columnar stromatolites (yellow field centimeter scale marked 20 cm). **(B)** Similar structure but more pancake-like. The vertical position of the dark colored columnar digitate stromatolites is showing finger-like structures with fine microfabric laminations. A closer field view of this type of laminations is shown in **(E)**. **(C)** Levels a, b, and c1. The lower level a consists of branching columnar digitate stromatolite; the level b shows reworked clasts (white arrow, probably tempestite) cutting the level a, and is overlain by thicker thrombolite below the level c1. **(D)** Buildup made of microbial vertical columns (2) growing on a thrombolite core (1). Yellow field scale, 20 cm. **(E)** Detailed field view of dark laminated microbial branching columns in a light lime mud matrix. Yellow millimetric field scale, 20 cm. **(F)** Level b, c1, and c2. The level b shows a core structure (1), support of fine branching columnar stromatolite partly bent (2), or straight (3). Levels c1 and c2 are occupied by botryoidal fanning digitate stromatolite columns (4); some above the core structure (1). **(B)** Upper right yellow field centimetric scale, 20 cm.

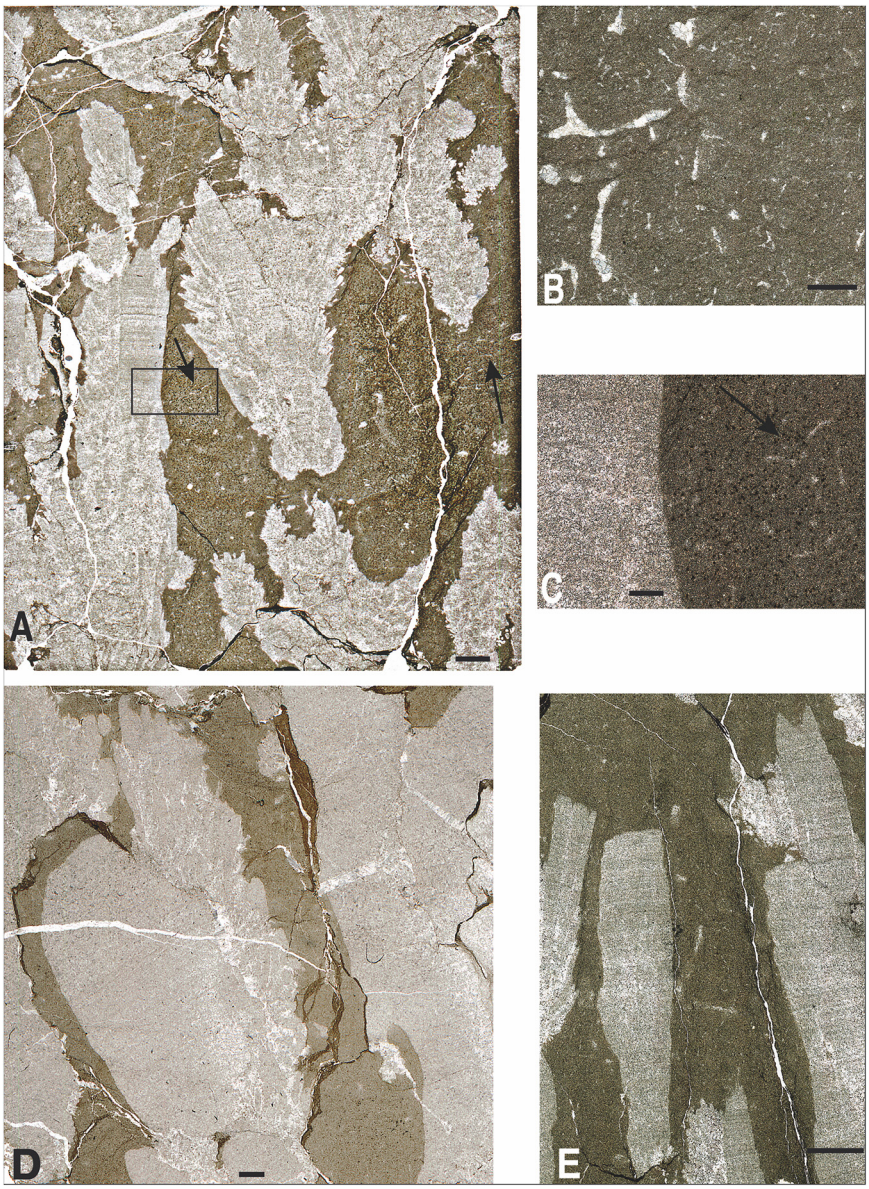

FIGURE 5 | Photomicrographs of thin sections from Abadeh, levels a to c. **(A)** Photomicrograph (sample Ha 6, level a) of digitate stromatolite columns (light) with local spray of calcite pseudomorph from aragonite crystal overgrowths in dark lime mudstone-fine packstone matrix with sponge fibers (arrow), scale bar–1 mm; **(B)** Enlarged view of the calcified keratose sponge fibers or spicules, scale bar = 200 μm (sample Ha 6, level a). **(C)** Enlarged rectangle from **(A)**: part of laminated column of digitate stromatolite with dark lime mudstone-fine packstone matrix with sponge fibers) on the right, scale bar 200 μm (sample IKH 76, level c1). **(D)** Finely laminated stromatolite columns (light) with local spray on the side of the calcite pseudomorphs replacing aragonite needle crystal overgrowths in dark lime mudstone-fine packstone matrix with rare sponge fibers, scale bar = 1 mm (sample Ha8, level c2). **(E)** Stromatolite columns (light) with local spray on the side of the fine calcite pseudomorph from aragonite crystal overgrowths in dark lime mudstone-fine packstone matrix with sponge fibers, scale bar = 1 mm (sample Ha7, level b).

The Shahreza Section: Sponge-Microbial Mounds and Aragonite Crystal Fan or Bundle Layers

The SMB succession of the Shahreza section is quite different from that of the Kuh-e Hambast sections. The mounds are not concentrated at the base but crop out over the first 20 m of the section within five main layers, SMB1 to SMB5 (**Figures 3A,B**, **6**).

–The first one (**SMB1**, **Figures 6.1**, **7A**) occurs in the lower boundary clay (level as in **Figure 6A**, **Figure 7A-3**), 0.6 m above his base, within the post-extinction interval of the upper *Clarkina meishanensis* conodont assemblage (latest Permian) and just below the earliest Induan *Hindeodus parvus* conodont Zone. Elongated crystal bundles (micro-calcite pseudomorphs of original aragonite crystals) were observed sprouting in a red, bioturbated mudstone matrix (Richoz et al., 2010).

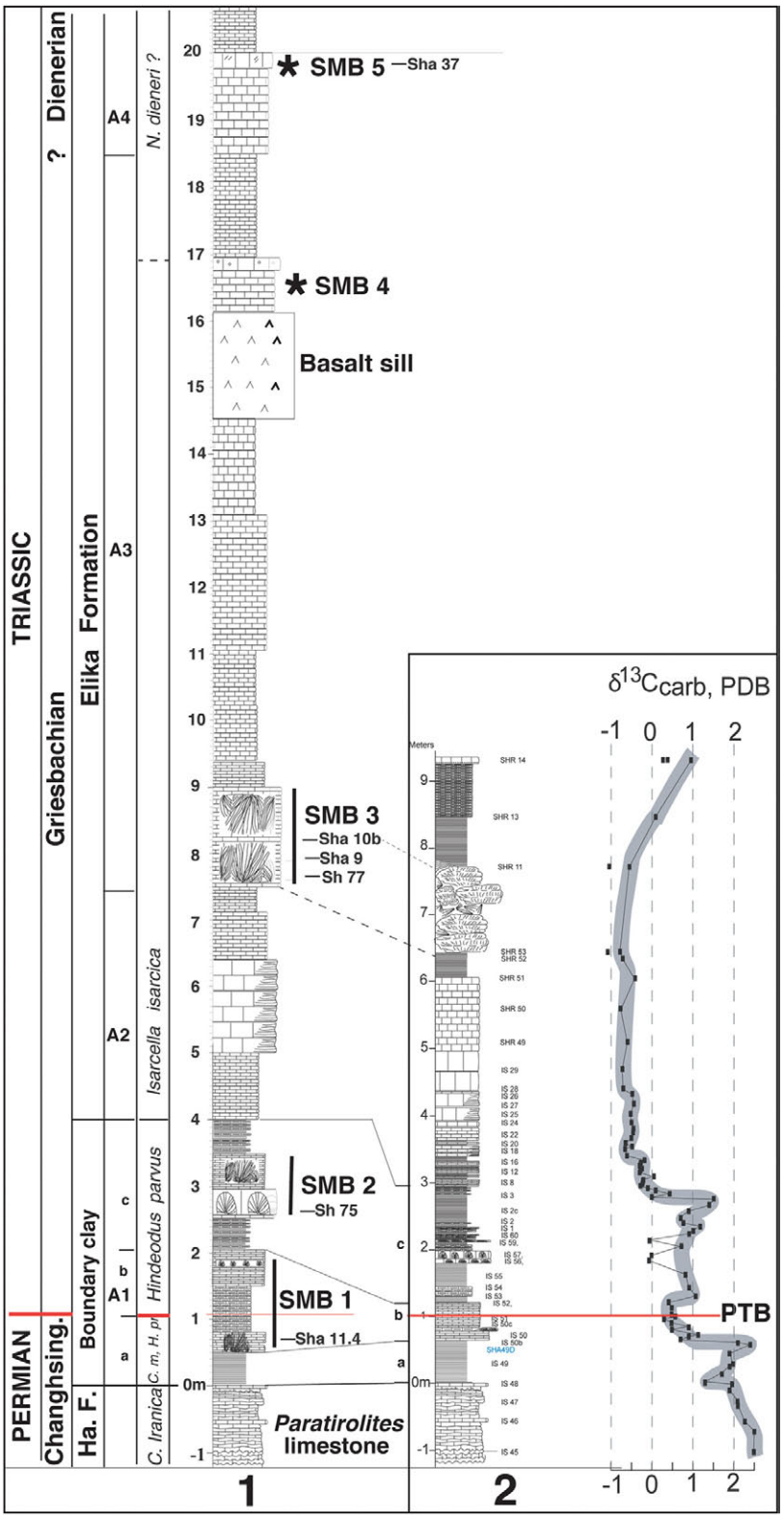

FIGURE 6 | Shahreza sections. **(1)** Composite section showing the position of the sponge-microbial buildup levels SMB1 to SMB5 and the samples Sh or Sha with thin sections illustrated in **Figures 7–11**; **(2)** Carbon isotope stratigraphy across the PTB (Richoz, 2006). The boundary clay (level A1, about 3 m thick) is subdivided into 3 parts (a = lower BC, b = middle, limy BC, c = upper BC), with the lower BC corresponding to the BC in Kuh-e Hambast. Ha. F.: Hambast Formation, Changhsing.: Changhsingian; C.: *Carkina*; H.: *Hindeodus*; m.p.- *meishanensis-praeparvus*; N.: *Neospathodus* (Kozur, 2005; Richoz et al., 2010).* :position of SMB4 and SMB5.

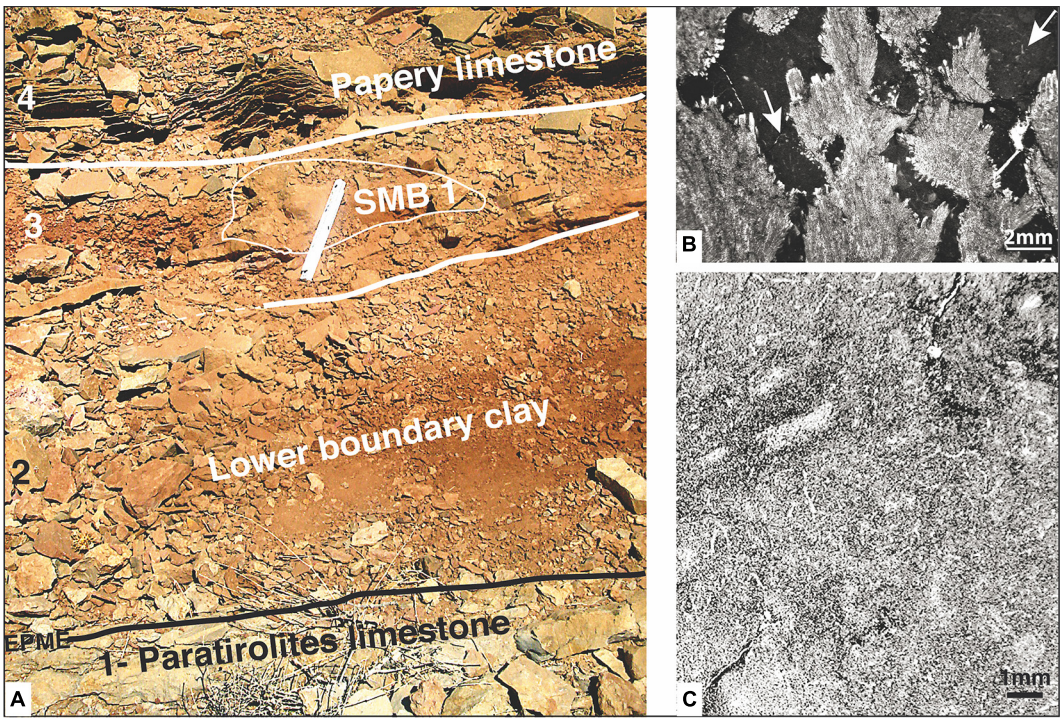

FIGURE 7 | Field view and photomicrographs, SMB 1 level at the Shahreza section. **(A)** Lower boundary clay field view (white field scale on SMB1 mound = 20 cm): 1- the top of the *Paratirolites* limestone corresponds to the end-Permian mass extinction (EPME); 2, Lower boundary clay, latest Permian in age (**Figure 3C** and level A1-a in **Figure 6.1**); 3, the first small mound (SMB1) within clay and marly limestone; the PTB is estimated chemostratigraphicaly to be at this level (see text); 4, papery limestone at the base of the upper boundary clay and close to the PTB (**Figure 3C** and level A1 -b in **Figure 6.1**). **(B)** Photomicrograph of the overgrown calcite pseudomorphs of aragonite crystal bundles in dark lime mudstone matrix with some sponge fibers (arrows; sample 11.4 in **Figure 6.1**). **(C)** Photomicrograph of a mesh of sponge fibers or spicules, possible keratose, with branching and fiber sections (sample ISH 50, laterally to SMB1 mound).

The microphotograph (**Figure 7B**) shows light gray microbial branching columns with aragonite crystal outgrowths replaced by calcite in a dark lime mudstone matrix containing spicules or sponge fibers. According to the microscopic views (**Figure 7C**), the finely recrystallized matrix of the surrounding lime mudstone is filled by a sponge fiber meshwork of possible keratose demosponge. This meshwork corresponds to the "sponge packstone" of Leda et al. (2014, their Figure 12B) at the same post-extinction level in Ali Bashi.

-The next higher sponge-microbialite layer **SMB2** (**Figures 6.1**, **8A–C**) occurs within the *Hindeodus parvus* conodont Zone and the next SMB3 level belongs to the *Isarcicella isarcica* conodont Zone (Richoz et al., 2010).

At 2.5 m above the base of the boundary clay, the SMB2a layer (**Figure 8A**) is about 10 cm thick and consists of open bowl-shaped fanning stromatolites columns. A detailed view is shown in **Figures 8B,C**. The microfacies of **Figure 8D** shows micro-laminated columns of digitate stromatolites lying above a leiolite type core (Sh 75 sample). This microfacies is similar to the lower SMB described and demonstrated in South Armenia (Sahakyan et al., 2017; Friesenbichler et al., 2018), and corresponds to the layer described by Baud et al. (2007, Figure 4A).

-Between 6.2 and 7.4 m above the base of the boundary clay, the **SMB3** level (**Figures 3B,C**, **9**, **10**) consists of a string in the region of 12 mounds of various thickness and structures within a distance of 200 m (**Figure 3B**). The largest one (3a, in **Figures 3C**, **9A**) that was illustrated earlier (Heydari et al., 2008) consists of well-preserved fans of elongated (10–15 cm) pseudomorphs of needle-like aragonite crystals, without visible laminations growing in free space and absence of surrounding sponge lime mud (**Figures 9B,C**). This abiotic mound type is unique (Baud et al., 2007, **Figures 4D,E**) and obviously does not exist in other central parts of Iran. A microphotograph of this lithoherm (Sha 10b, **Figure 9D**) shows only calcite microsparite of diagenetically altered fanning aragonite needle-like crystals.

This SMB was possibly a sponge microbial mound originally, as well as others in close proximity. The high, well-connected porosity, and hydrothermal fluids that occurred during the later basaltic intrusion could possibly have caused the observed special recrystallization in decametric long needle-like aragonite crystal fans, which is now regarded as calcite microsparite at photomicrograph scale. Further geochemical studies might provide a solution.

All other mounds of the SMB3 level originated from sponge-microbial with partly thrombolitic mesostructures exhibiting various shapes, as can be seen in **Figures 10A,D**. The largest one, 2.5 m in length and 0.8 m high, consists of about ten decimetric superposed mounds of partly thrombolite type, some with domal structure (**Figure 10A**). A detail view of one of these mounds shows a fanning structure of distinct lath shaped,

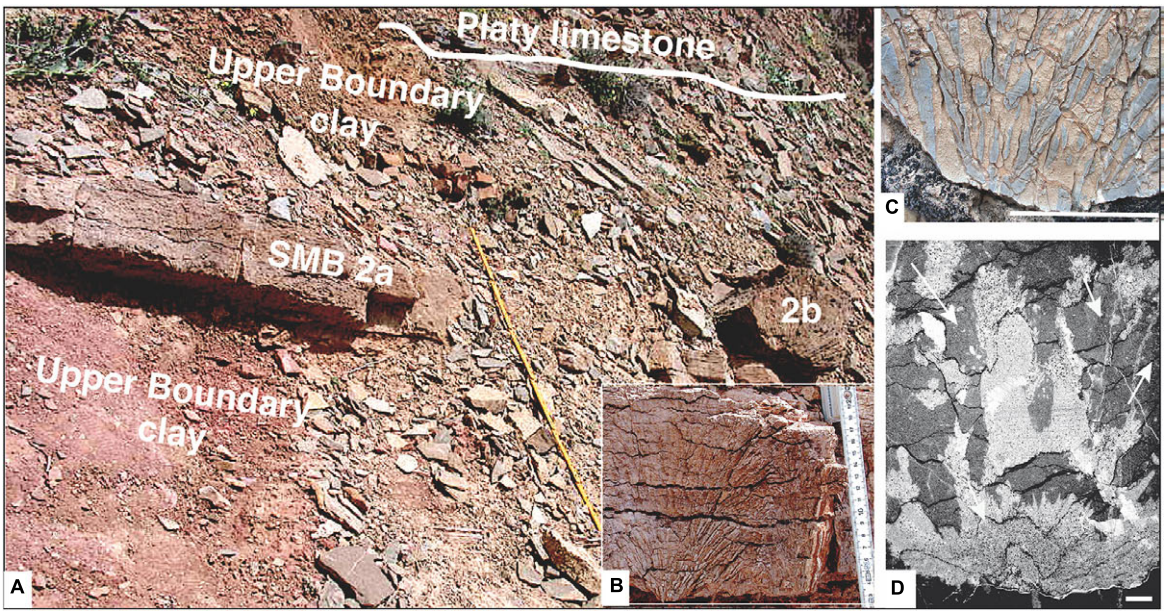

FIGURE 8 | Field view and photomicrographs, SMB 2 level at the Shahreza section. **(A)** General overview of the SMB2a within the upper boundary clay (level A1c in **Figure 11**) and the base of the platy limestone (2b is a loose block; yellow field centimeter scale: 1, 20 m). **(B)** Detailed view of the SMB2a with the fan-shaped digitate stromatolite columns. **(C)** Another detailed view of the basal part of a SMB showing the shrubby type of the light gray branching columnar stromatolite with visible fine laminae (white scale bar = 5 cm). These fine vertical growing stromatolites are very similar to those illustrated by Yang et al. (2019), **Figures 4A–D**. **(D)** Photomicrograph of light micro-laminated columns of digitate stromatolites above a leiolite type core in dark lime mudstone matrix with sponge fibers (white arrows, sample Sh 75 in **Figure 6.1**, white scale bar = 1 mm).

finely laminated stromatolite columns (**Figure 10B**). Microfacies highlights the growth of encrusting calcite crystals directly on the laminated stromatolite columns (**Figure 10C**). Another, the SMB3b buildup of an inverted conical structure, is made of five vertically superposed thrombolite plates from 10 to 54 cm in diameter at the top and of 1 m total high (**Figure 10D**). The microfacies of the thrombolite shows mesoclots surrounded by a dark lime mud matrix with some sponge fibers as can be seen in **Figure 10E**.

-Between the range of 16 and 20 m above the boundary clay, there are at least two more microbial layers, SMB4 and SMB5. Similar to SMB5 the **SMB4** is not illustrated here.

-A sponge-microbial mound of level **SMB5** showing dark patches of spheroid clots on top of the outcrop domes is shown in **Figure 11A**. The microfacies consists of micro-sparitic patches of the leiolite type and coalescent spheroids in a dark lime mudstone matrix with sponge fibers (**Figure 11B**). **Figure 11C** shows an enlarged inverted gray view of a small part of a spheroid filament network (part underlined in red). This arrangement clearly looks like fibrous tissue of keratose demosponges, which is in consonance with Luo and Reitner findings Luo and Reitner (2014, Figure 4). Sponges and microbialite (leiolite) are both involved in the buildup growth.

DISCUSSION

Three main debates are presented below, sponge takeover following EPME, biotic or abiotic carbonate mounds and biochronology of the Permian-Triassic boundary. Comparisons with the nearby Baghuk Mountain section and with the Ali Bashi and Zal sections (NW Iran) close this chapter.

A Sponge Takeover?

Shapiro and Awramik (2006) described Cambrian age sponge-microbial bioherms in New York State, United States and Coulson and Brand (2016) demonstrated Cambrian lithistid sponge-microbial reef-building communities in SW Utah, United States. For these authors, the sponge microbial bioherms have largely remained unnoticed due to the size of the sponges and the cryptic method of preservation.

Friesenbichler et al. (2018) described sponge microbial bioherms for the first time in South Armenia and differentiated four facies (Sponge Facies 1–4) based on the spicule isolate forms or the fibers forming network.

Here, the sponge fibers illustrated in **Figures 5B,C**, **7F,G**, correspond to the "Sponge Facies" and "sponge spike" of Leda et al. (2014). Smaller spicules, as seen in the matrix of **Figure 9E**, can be compared to the Sponge Facies 2. The larger ones as seen in the dark matrix of **Figure 10C**, correspond to Sponge Facies 4. The texture of the coalescent spheroids illustrated in **Figure 10C** corresponds better to the young (Smithian) sponge facies described and illustrated by Brayard et al. (2011, supplementary information). Luo et al. (2014), Luo (2015), and Luo and Reitner (2016) identified these structures in tiny sections as potential remains of keratose sponge fibers. As shown by Lee and Hong (2019), the keratose-like sponges

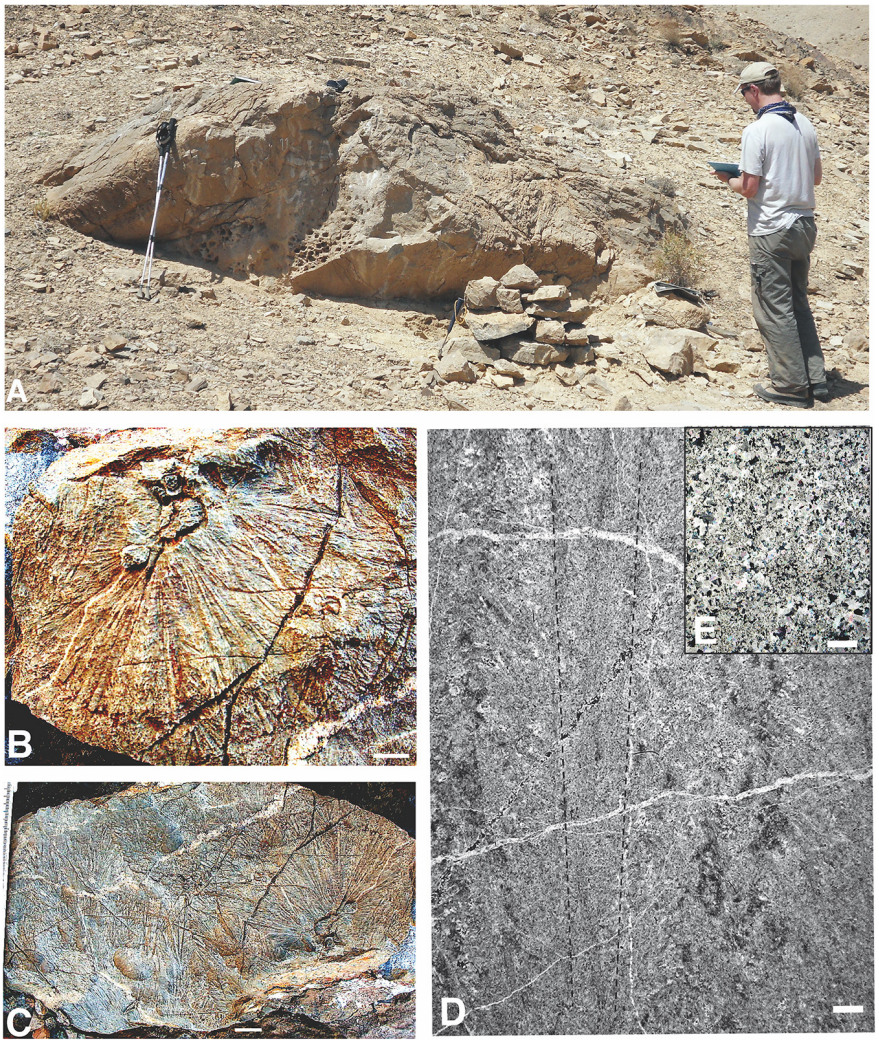

FIGURE 9 | Three outcrop views and a photomicrograph of the lithoherm SMB3a within the SMB3 level at the Shahreza section. **(A)** General view of the crystal lithoherm mound (height-180 cm). **(B,C)** Outcrop surface details: decimetric long needle-like calcite crystal fans, possibly of aragonite origin (white scale bar = 1 cm). **(D,E)** Photomicrographs. **(D)** Is showing diagenetically altered micro-sparitic calcite crystals (sample Sha 10b, white scale bar = 1 mm) originally of fanning aragonite needle-like crystals. **(E)** Enlarged view of the micro-sparitic calcite crystals in polarized light (sample Sha 10b, white scale bar = 200 μm).

often/usually co-exist with microbialites and act as stabilizers of the reef framework.

Additionally, the presence of sponges in the basal Triassic has been identified outside the Cimmerian margin (South Armenia, Northwestern Iran, Central Iran) of the Neo-Tethys. On the Gondwana side of the Neo-Tethys, microbial-metazoan bioherms of the basal Triassic Kuh-e Surmeh section in the Zagros and the Cürück Dagh section in the Western Taurus (Turkey) showed significant contributions of possible keratose sponges (Heindel et al., 2018; Foster et al., 2019).

In the post-EPME successions of South China, sponge remains have been reported in only very few sections so far due to their cryptic preservation potential. One of these sections is the Langpai section (Guizou) where "sponge-like fabrics" were reported by Ezaki et al. (2008, Figure 8C), another is the Shanggan section (Guangxi) with stromatactis buildups that originated from sponge-microbial, as described by Baud et al. (2013).

In modern reef settings, it is not uncommon for sponges to initially colonize areas vacated by metazoans (Brunton and Dixon, 1994). According to Foster et al. (2019), the post-EPME keratose sponges recorded in South Armenia and Iran sections were interpreted as r-strategists. During "background times," they also occur in association with microbialites and are limited to settings associated with less favorable environmental conditions.

Corsetti et al. (2015) also suggested a "sponge takeover" after the end-Triassic extinction period. We hypothesized here that the post-EPME "sponge takeover" resulted from the unique situation of environmental circumstances in the aftermath of the end-Permian mass-extinction and that the sponge event recorded along the Cimmerian margin and along the Gondwana margin of

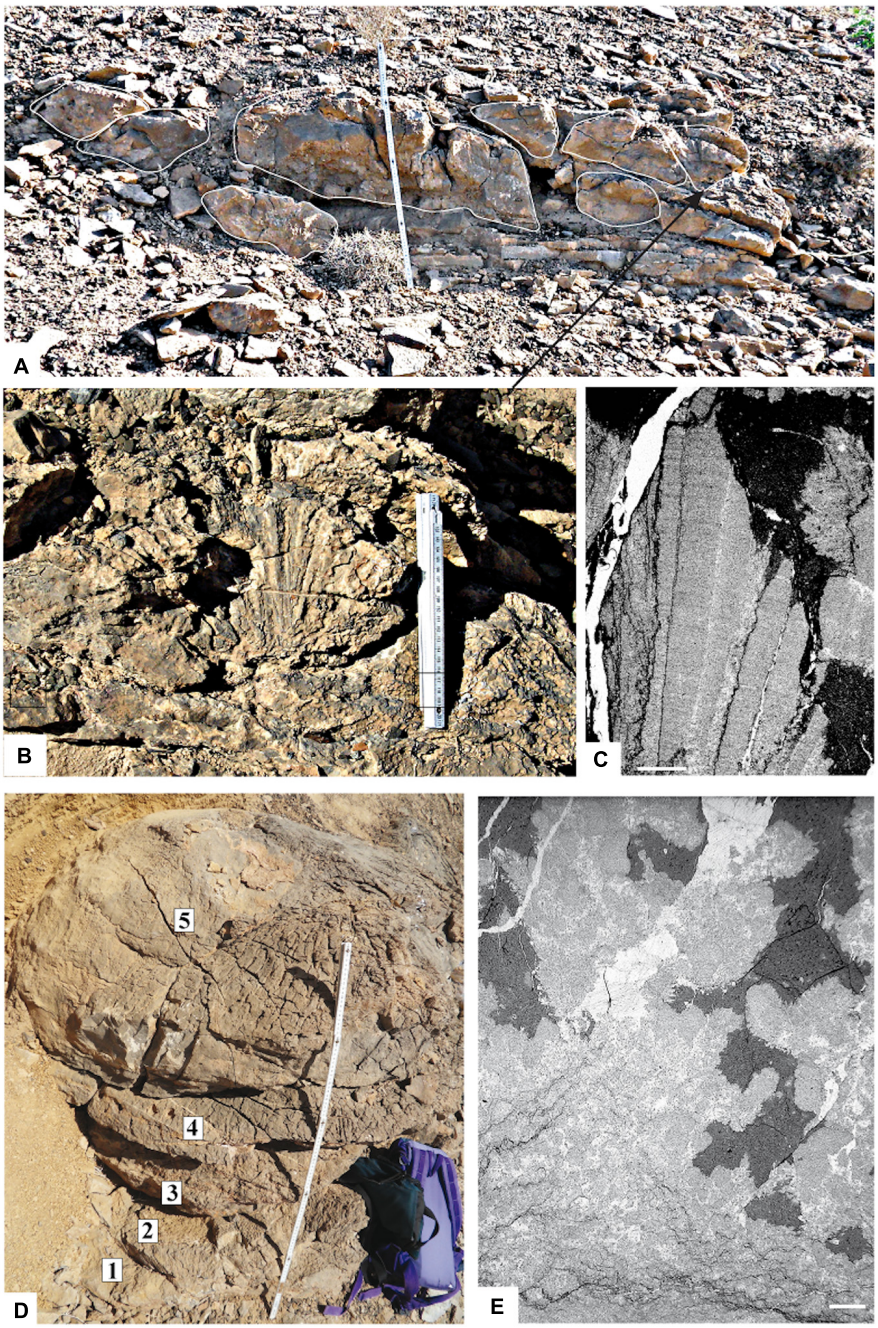

FIGURE 10 | Three outcrop views of a complex sponge-microbial buildup of the SMB3 level with photomicrographs in the Shahreza section. **(A)** Field view of the 50 cm thick complex layout of mounds within the platy limestone (white field, 80 cm scale). **(B)** Detailed view of mound fan-shaped digitate stromatolite columns (white field, 20 cm scale). **(C)** Photomicrograph of lath-shaped, finely laminated stromatolite columns, partly replaced by calcite mono-crystals in a dark lime mudstone to fine packstone matrix (sample Sh 77, white scale bar = 1 mm). **(D)** Outcrop view of the 1 m high (field scale) SMB3b mound, composed of five thrombolite plates (1–5, 40 cm in diameter at the top). **(E)** Photomicrograph of thrombolite mesoclots (light) in dark lime mudstone to fine packstone matrix with some sponge fibers (sample Sha 9, white scale bar = 1 mm).

the Western Neo-Tethys appear to have been a response to both ecological and geochemical changes.

Sponge-rich bioherms, which developed first in the Western Neo-Tethys during early Induan time as shown here, became later widespread in the Western US Panthalassa margin during the Olenekian as demonstrated by Griffin et al. (2010) and by Marenco et al. (2012). Brayard et al. (2011) and Vennin et al. (2015) presented in Pahvent Range and Mineral Mountains (Utah) new evidence for large *in situ* early Smithian to middle Spathian metazoan bioaccumulations, and reefs formed by

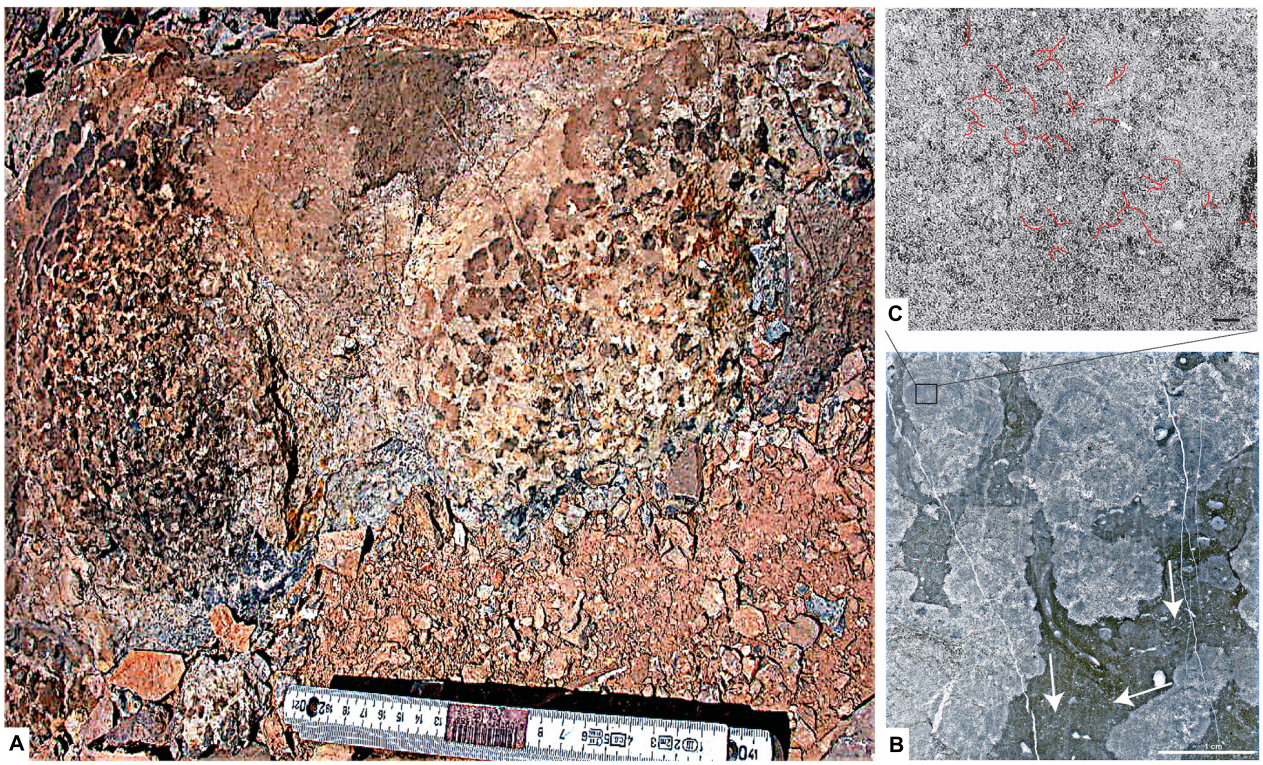

FIGURE 11 | Outcrop view of the SMB5 level and photomicrographs in the Shahreza section. **(A)** Top of mound showing dark clots in light lime mud matrix (white field centimeter scale). **(B)** Photomicrograph showing light gray micro-sparitic patches of both thrombolite and coalescent spheroids (sponges?) within dark lime mudstone to fine packstone matrix with sponge fibers (arrows, sample Sha 37, white scale bar = 1 cm). **(C)** Enlarged inverted gray view (rectangle in **B**, upper left corner) showing a possibly calcified network of sponge fibers (underlined in red, sample Sha 37, black scale bar = 1 mm).

various sponges, as well as serpulids associated with different microbial carbonates and eukaryotic organisms with at least two different classes of sponges (*Demospongiae* and *Calcarea*) supporting a multi-species sponge community.

In Oman, lower Olenekian red microbial stromatactis limestone (Woods and Baud, 2008) that are rich in sponge spicules found around small cavities (Baud and Richoz, 2013) and a Smithian giant reef block with sponges is under investigation.

We also have to note that J. Szulc was the first to introduce the Lower Triassic sponge-microbial reef recovery concept (Szulc, 2003, 2007, 2010), even though he only presented short notes on shallow water carbonates from the Carpathian area.

Crystal Fans, Carbonate Crust, Digitate Microbialite, or Digitate Stromatolites?

Our illustrated sponge-microbial bioherms in Abadeh and/or Shahreza have been described in the past with a great variety of terminology such as laminated microbialite structures (Taraz et al., 1981; Figure 11 = algal biolithite), dendrolite (Richoz, 2006), digitate or branching stromatolites (Baud et al., 2007; Richoz et al., 2010), inorganic fan-shaped calcite crystals (Heydari et al., 2003; Horacek et al., 2007b) and carbonate crust (Mette, 2008).

Working on similar structures in the Chanakhchi section in South Armenia, Friesenbichler et al. (2018) clarified the microbial origin of the fine, regular and slightly wavy laminations. The origin was demonstrated by weak transmitted luminescence and UV light in Figures 6A,B of their research article. The cathodoluminescence study of Friesenbichler et al. (2016) shows a non-uniform bright orange and red luminescence illumination on the branches. Same observations were reported by Leda et al. (2014, p. 315) on laminated calcite "crystals" of Abadeh and Baghuk Mountain sections. This luminescence has its source in the organically formed, microbial part of the laminated branches. It is why the term of digitate stromatolite has been used by Friesenbichler et al. (2018).

On our side, we have identified in the field that the digitate structure predominantly shows a parallel (**Figures 4B,E**) or a fan-like arrangement (**Figures 4A**, **7B,C**, **9B**) and that branches or columns are showing a fine laminated texture (**Figures 4B,E**, **8C**). A fine wavy stromatolitic fabric of the vertical branches is clear in the corresponding microphotographs (**Figures 5A,D,E**, **9C**). Accordingly, we also use the descriptive digitate stromatolite term here.

The sprays of aragonite pseudomorph on the side of the stromatolitic branches did not show any fluorescence and were interpreted as abiotic overgrowth (Friesenbichler et al., 2018).

In this study, in agreement with Friesenbichler et al. (2018), we used the phrase "calcium carbonate crystal fans" in a descriptive sense to refer to the mesostructural scale and not as a genetic notion that implies an abiotic origin (e.g., Grotzinger and Knoll,

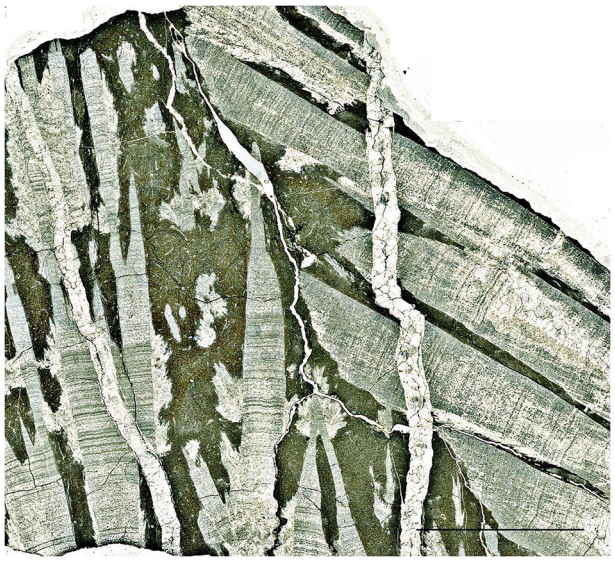

FIGURE 12 | The basal Triassic SMB of the Armenian Vedi section; thin section scan view. The vertical and the tilted structures of coalescent columnar stromatolites are replaced by a direct growth of encrusting calcite crystals with rare calcified acicular aragonite crystals at the side, in a dark lime mud matrix rich in calcified sponge fibers. Scale bar, 1 cm.

1995; Woods et al., 1999, 2007; Heydari et al., 2003; Pruss et al., 2006; Riding, 2008). The CCFs in Central Iran display mainly two components in a dark lime matrix:

(1) Elongated calcium carbonate aggregates mimicking a crystal shape with a high length-to-width ratio and almost straight but slightly wavy margins; referred to as digitate stromatolites in this study.

(2) A local spray of calcite pseudomorph from aragonite crystals growth on the side of the branches, confirmed as abiotic calcium carbonate crystal fans in this study.

But this phrase "calcium carbonate crystal fans" was used in a genetic and abiotic sense by Heydari et al. (2003) and Leda et al. (2014, p. 319). These last authors stated that "the internal lamination of the calcite fan branches is intriguing and cannot be explained easily by inorganic spontaneous calcite crystal growth on the sea floor." It is important to note that what looks like pseudomorphs of elongated calcite crystals at first glance, and which was documented at the Baghuk Mountains (Leda et al., 2014; Figures 12E,F) corresponds exactly to our digitate stromatolites (**Figures 5A,E**) and the ones from the Chanakhchi section described by Baud et al. (2015) and Friesenbichler et al. (2018, Figures 5A,C), as well as the fanning structures, about 10 cm in height of the coalescent digitate stromatolites (**Figure 12**) from the Vedi sections (South Armenia, Sahakyan et al., 2017).

In the Shahreza section, we noted that Heydari et al. (2003) focused on the study of only one mound (indicated as 3a in **Figures 3C**, **8A**) and apparently overlooked the microbial structure of other mounds in this section. The interpretation of this structure (Mound 3a) as carbonate seafloor precipitates made Heydari et al. (2003) to claim that they were formed from $CaCO_3$ oversaturated seawater due to sea level fall in oxic environment. This interpretation was challenged by Wignall et al. (2005), who disproved the oxic environment interpretation, and Zong-jie (2005) who interpreted these structures as microbialite crusts produced in anoxic environment without evidence for a sea level change. Our results are at variance with Heydari et al. (2003) model and their contradictors as well as Foster et al. (2019), indicating, due to pyrite framboid arguments, that both Shahreza and Abadeh were deposited in an oxic environment. Even though abiotic precipitation of carbonate did occur, most of the carbonate precipitation was however microbial-mediated. Certainly, there was carbonate oversaturation at that time but not up to the amount proposed by Heydari et al. (2003). As stated before, further geochemical studies might provide a solution for the Mound 3a perhaps/probably due to a proximal basalt sill influence.

The fabric of digitate structures (**Figures 4A,D**, **7B,C**, **9B,C**), or mounds made of typical thrombolite plates (**Figure 9D**) and domes covered by microbial dark patches of spheroid clots as shown in **Figure 10A** have been previously ignored or misinterpreted. In all the corresponding microfacies, a lime mud matrix (lime-mudstone or fine wackestone) exposed calcified sponge fibers or spicules (**Figures 5**, **7E–G**, **9C,E**, **10B,C**); all of which are typical of SMBs.

Looking in other areas, similar digitate structures of the same age and containing fine columnar laminations are described from Tieshikou in South China (Yang et al., 2019). The authors use the terms of digitate microbialites, of laminated columns and of microstromatolite grew. But in the Chongyang sections (South China) Wang et al. (2019) use the term of columnar stromatolite in their Figure 6 of laminated columns and wrote about digitate structure. Both sections belong to shallower depositional environment with smaller columnar sizes and apparently lack associated sponges.

Biochronology

An introduction to the biochronologic debate on the Permian-Triassic boundary is presented in section "Introduction." (Korte et al., 2004a,b) and Kozur (2005, Figure 3), in contrary to previous work by Taraz et al. (1981) and Gallet et al. (2000), reported only 0.5 m of microbialite and the first occurrence of *H. parvus* 1.2 m above the *Paratirolites* limestone. This 1.2 m position is above the datum proposed earlier by Taraz et al. (1981) and Gallet et al. (2000) at 0.3 m above the *Paratirolites* limestone. The lower datum was confirmed later by Richoz et al. (2010, plate 2).

Successive studies by Shen and Mei (2010) and Chen et al. (2020) use the PTB-finding of Kozur (2005), whereas Shen et al. (2013) and Dudás et al. (2017) followed the scheme proposed by Taraz et al. (1981), Gallet et al. (2000), and Richoz et al. (2010). Here we also use the Permian-Triassic boundary defined by the latter group at the base of the microbialite in the Kuh e Hambast sections of Abadeh. For a full discussion of the PTB-problem at Abadeh please refer to Horacek et al., 2021.

At the Shahreza section, the boundary clay interval is thicker, about 4 m in the composite section (**Figure 6.1**), and 3 m in the sampled section (**Figure 6.2**), which is further subdivided

into three parts, with papery limestone beds and small sponge-microbial mounds in between (**Figures 6.1**, **7A**). Kozur (2005) demonstrated that the basal Triassic conodont assemblage starts from the lower part of the upper boundary clay, about 1.6 m above the base of the boundary clay. However, Richoz (2006) and Richoz et al. (2010) proposed moving the PTB, which was 0.6 m lower, to 1 m above the base of the boundary clay, based on chemostratigraphic evidence ($\delta^{13}C_{carb}$ curve). The boundary clay in Kuh-e Hambast correspond thus to the lower part of the boundary clay in Shahreza.

At the Kuh-e Hambast section, the first Dienerian conodont zone starts at the 17 m mark above the extinction level (Taraz et al., 1981, p. 91). Considering similar depositional rates in Baghuk, Shahreza and Abadeh sections, the upper SMB5 would likely occur around the early Dienerian time. In the Abadeh sections the microbialites are restricted to the early Griesbachian, whereas in Shahreza the SMBs are composed of some irregularly spaced sponge-microbial buildups with different sizes and various external morphologies and internal structures up to the early Dienerian. The Shahreza SMBs are very similar to the South Armenia SMBs succession published by Friesenbichler (2016); Friesenbichler et al. (2018).

Depositional Environment

According to Leda et al. (2014), the Changhsingian *Paratirolites* limestone and the overlying Induan platy limestone (Elika Formation) of Ali Bashi section were deposited in the open sea dysphotic zone below the storm wave base at a depth of about 100–200 m. The NW Iran sections (Zal, Ali Bashi) were estimated to have been deposited at distal ramp, about 250–500 m in depth for *Paratirolites* beds (Aghai et al., 2009). However, in Central Iran we saw evidence of a shallower depth, about 60 m, in a ramp environment close to storm wave base, due to the presence of distal tempestites in the SMBs of Abadeh (**Figure 4C**, level b).

The marly boundary clay still contains carbonate but greatly reduced with respect to the underlying and overlying limestone successions (Joachimski et al., 2020). This implies that the production of carbonate was drastically disrupted due to the EPME and massive fluctuations between carbonate undersaturation and supersaturation, as elucidated by Leda et al. (2014).

Comparison With the Close Baghuk Mountain Section

Situated 77 km SE of Shahreza section (**Figure 1**), section C of the Baghuk Mountains (Coord.: 31° 34' 4.73" N, 52° 26' 37.69" E) was recently described by Leda et al. (2014), Foster et al. (2019), and Heuer et al. (2017, Submitted). The first publication gave details mainly on the end-Permian *Paratirolites* limestone and the boundary clay units. The second article gave a short description of basal Triassic platy limestone and the discovered microbialite units. It is interesting to note that the microbial levels in the Baghuk section are found in the same position as the SMB in the Shahreza section (**Figure 13**). This is buttressed by the presence of a 1.6 m thick basalt sill level in this section.

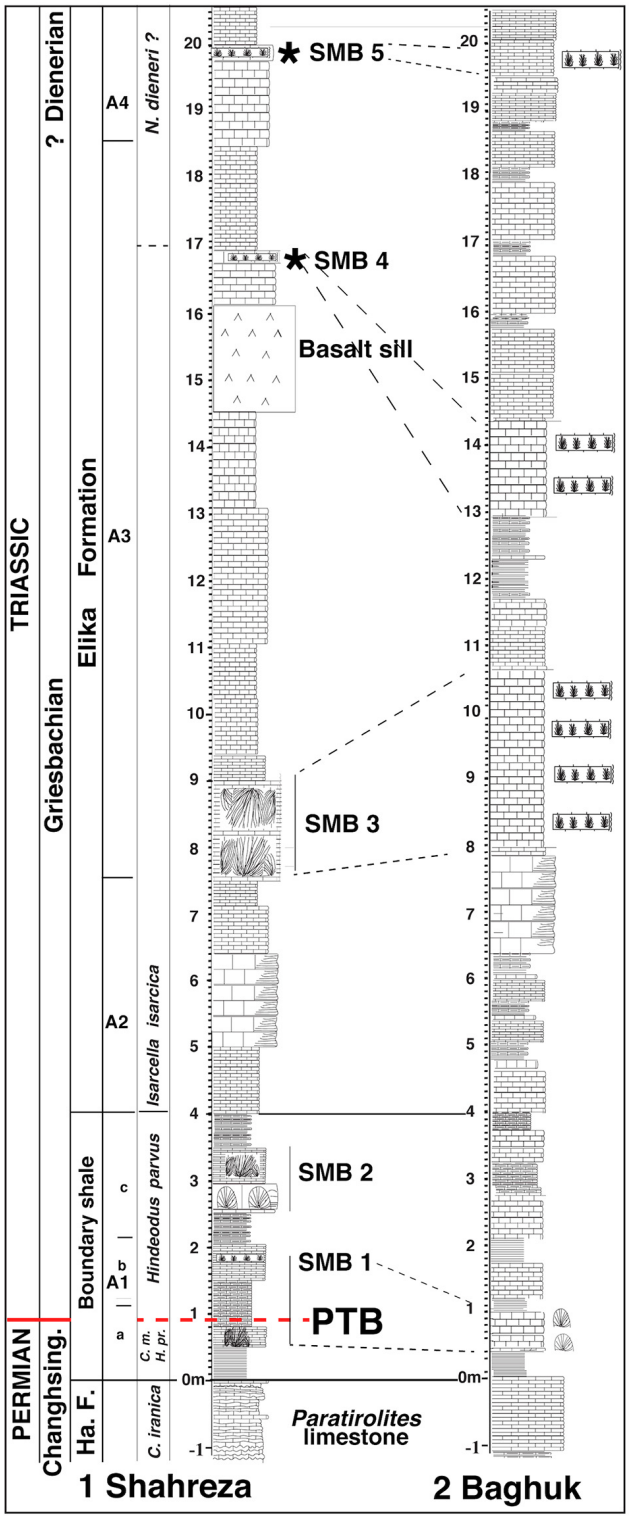

FIGURE 13 | Correlation between the Shahreza and the Baghuk Mountain section based on thickness and SMB occurrences. **(1)** Stratigraphy of the Shahreza section showing the position of the sponge-microbial buildup levels SMB1 to SMB5 (see caption of **Figure 6** for abbreviations and references). **(2)** A sketch of the Baghuk Mountain section showing the position of the four main mounds levels modified from Heuer et al. (2017).

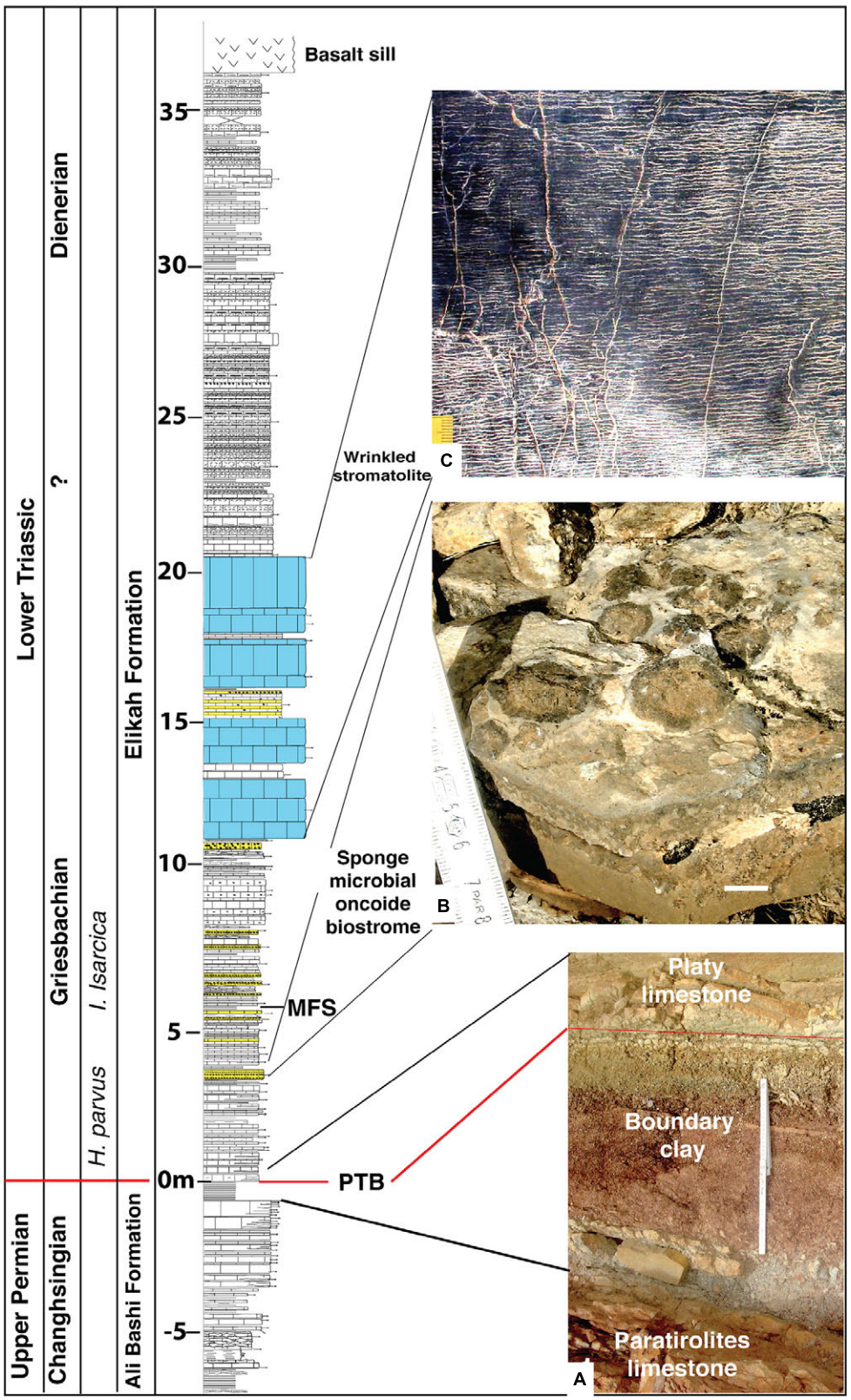

FIGURE 14 | The Zal section, modified from Richoz (2006). PTB = Permian-Triassic Boundary; MFS = Main Flooding Surface; decimeter thick bedded biostromes (yellow) and wrinkled stromatolite (blue color). **(A)** View of the boundary clay, 60 cm thick (white field, scale 40 cm). **(B)** Bed surface with 1–2 cm large spheroid sponges (white scale bar 40 cm). **(C)** Laminated gray limestone with "wrinkle"-structure (yellow field scale 1.5 cm).

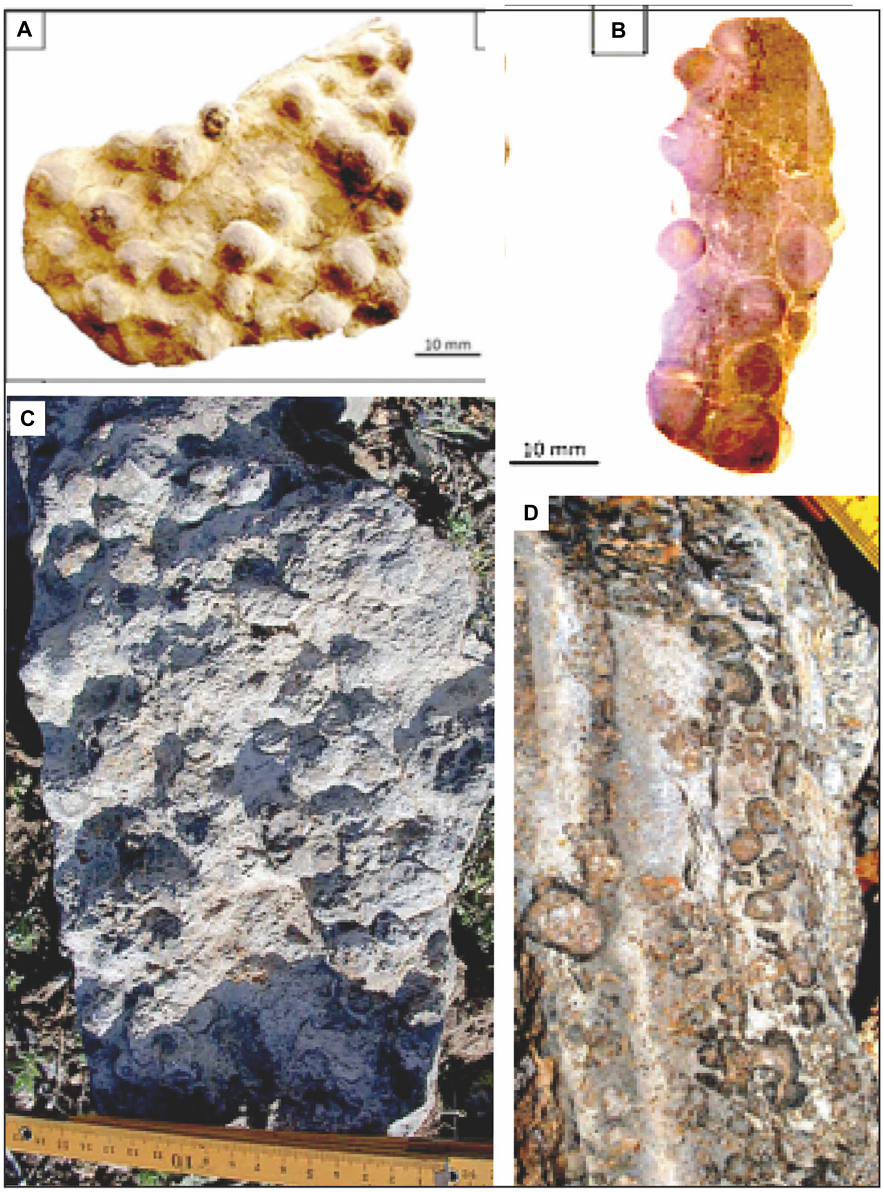

FIGURE 15 | Comparison between macroscopic view of spheroid sponges. **(A,B)** Smithian unit of Mineral Mountains (Utah, United States) illustrated by Brayard et al. (2011), in their Supplementary Figure 5. **(C,D)** Potential spheroid sponges from the Griesbachian of the Zal section. **(A,C)** Upper surface. **(B,D)** Transverse section, yellow field scale in upper right corner ca 1.5 cm.

As in the Shahreza section, the mesh of algal filaments in the matrix of the Baghuk section boundary shale has been interpreted as a remainder of sponge spicules by Leda et al. (2014, their Figure 12B), and by Heuer et al. (2017, Submitted). These authors also identified in Ali Bashi a sponge packstone called "sponge spike" at the top of the end-Permian *Paratirolites* limestone with predominant triaxon-like morphologies. However, due to the poor preservation of the sponge remains, detailed description could not be given. According to Luo and Reitner (2014), the so-called "mesh of filaments" consists of possible calcified keratose sponge organic fibers or tissues (spongin). Furthermore, similar pseudomorphs of elongated calcite crystals growing along branches in the Baghuk Mountain section (Leda et al., 2014, their Figures 12E,F) have been discussed in section "The Kuh-e Hambast C Section of the Abadeh Area." The dome-shaped structures described by Leda et al. (2014 p. 315) have been interpreted as microbialites by Heuer et al. (2017, Submitted). In **Figure 13**, we correlated it with our Shahreza sponge-microbial buildups (SMB).

The NW Iran PTB Sections Near Julfa

The NW Iran Ali Bashi and Aras Valley sections have been described in great detail by Leda et al. (2014) and Gliwa et al. (2020) and compared with Abadeh and Bahguk Mountain

sections. It is interesting to note the apparent absence of carbonate mounds and buildups in NW Iran platy limestone (called *Claraia* beds). Also, oncoidal facies have been identified in the Ali Bashi section, 2 m above the base of the *Claraia* beds (Leda et al., 2014), having the same age (*Isarcicella isarcica* conodont Zone) as the oncoids found in Abadeh.

The NW Iran PTB Zal Section

The Zal section is located about 23 km SSW of Julfa and in close proximity to the village of Zal (38° 43′ 59″ N, 45° 34′ 48″ E). Sedimentology and microfacies of the lower part of the section have been described in detail by Leda et al. (2014). Basal Triassic large oncoid bearing limestone was highlighted by Baud et al. (2007) and the litho-, bio- and chemostratigraphy of the entire Lower Triassic succession having a thickness of 750 m was published by Horacek et al. (2007a) with detailed information on the Sr isotope record described by Sedlacek et al. (2014), and the U isotope changes described by Zhang et al. (2018). A detailed description of the PTB interval relating to chemo- and biostratigraphy was published by Richoz (2006), Richoz et al. (2010), Schobben et al. (2014, 2015, 2016, 2017), and Wardlaw and Davydov (2005).

Unlike the mound or bioherm facies at the Shahreza and Abadeh sections, the Zal section (**Figure 14**) contains tens of decimetric thick bedded limestone (yellow colored portion in **Figure 14A**) and dark coalescent spheroids between oncoids (**Figure 14B**) located between 3 and 11 m above the boundary clay. The oncoids were well described by Leda et al. (2014, p. 313) in their study, where they described two varieties, R and C.

The dark coalescent spheroids (**Figure 14B**) are very similar to the spheroid sponges (**Figures 15A,B**) from the Smithian of Mineral Mountains (Utah, United States) described by Brayard et al. (2011, Figure 5) and the possible spheroid sponges from the Griesbachian of the Zal section described in our study (**Figures 15C,D**). Arnaud Brayard (written communication) was convinced by our comparative study highlighted in **Figure 15**. In this study, we interpreted the dark coalescent spheroids of Zal as possible sponges and the deposit as biostrome due to the observed presence of sponge fibers around the spheroids. They are overlain by thick bedded wrinkled lime laminated mats (**Figure 14C**). This will be described in another article (Brandner et al., in prep.).

CONCLUSION

A sponge takeover that started during the EPME in South Armenia and NW Iran has been confirmed in Central Iran sections and found to extend to the lower Griesbachian in the Kuh-e Hambast C sections and possibly up to Dienerian time in the Shahreza and Baghuk sections.

We argued that these permineralized remnants of keratose demosponges belong to a wide range of microbial mounds built in part by digitate stromatolite columns. With the same age, types and microfacies, these buildups correspond to those recently described in South Armenia (Sahakyan et al., 2017; Friesenbichler et al., 2018).

In the Kuh-e Hambast C section of the Abadeh area, these SMB are restricted to the 1.60 m thick interval of successive mounds showing numerous arborescent structures with decimeter-scale branching columnar stromatolites surrounded by lime mud rich in fibers of keratose-like sponges, and early Griesbachian in age (*Hindeodus parvus* conodont Zone). As asserted in the South Armenia studies, the calcium carbonate oversaturated seawater induced a very early diagenetic replacement of the previous digitate microbial organic tissue as of the demosponge fibers.

The Shahreza section showed five successively spaced SMB cropping out over the first 20 m of the section starting from the post-extinction latest Permian and ending at the early Dienerian thus spanning about 700-ky. The surrounding sediment and the thinly bedded platy lime mudstone characterizes an open marine distal ramp environment close to or below the storm wave base.

In this distal ramp environment, which is about 60 m deep, the SMB grew successfully with topographic reliefs above the seafloor. Therefore, an in-depth description of the post-EPME microbial-metazoan bioherms with branching and columnar stromatolite can be related to sponges cropping out along the Cimmerian margin of the Neo-Tethys in South Armenia and Central Iran.

DATA AVAILABILITY STATEMENT

The datasets presented in this study can be found in online repositories. The names of the repository/repositories and accession number(s) can be found below: Samples and thin sections are deposited at the Geological Museum, Bâtiment Anthropole, UNIL; CH 1015 Lausanne, Switzerland.

AUTHOR CONTRIBUTIONS

SR and AB designed the research. AB, SR, LK, RB, KH, MH, TM, and PM-A collected the field data and the samples. AB and SR carried out the sediment studies and facies analysis with the help of RB, LK, and KH and wrote the manuscript with the help of LK, RB, KH, and MH. All authors contributed to the article and approved the submitted version.

FUNDING

Field researches for this study was supported through the Austrian National Committee (Austrian Academy of Sciences) for IGCP, project IGCP 572, 630. NAAP0018.

ACKNOWLEDGMENTS

Fieldwork carried out in Iran in 2002 was supported by the Geological Survey of Iran (GSI). We are grateful to Drs. B. Hamdi, B. Momeni, and M. Vakil from the GSI and Dr. W. Mette from

Innsbruck University for their support during the fieldwork. We are grateful to the Geological Survey of Iran for logistic support during fieldwork in 2011. In particular, we wish to acknowledge Hamid Karimi for his assistance and encouragement. The grant for fieldwork in 2011 was awarded by the Austrian National Committee (Austrian Academy of Sciences) for IGCP: Project IGCP 572, NAAP0018. We also wish to appreciate several of our colleagues, especially Jonathan Payne who read an earlier version of the manuscript and gave valuable advice, positive feedback, encouragement, and highlighted areas that required improvements. We also appreciate recent constructive reviews by Dieter Korn and Zhong-Qiang Chen.

DEDICATION

In memory of Maurizio Gaetani, outstanding field geologist, scientist and friend.
In memory of Joachim Szulc, pioneer of the Lower Triassic sponge-microbial reef recovery concept.

REFERENCES

Aghai, P. M., Vachard, D., and Krainer, K. (2009). Transported foraminifera in palaeozoic deep red nodular limestones exemplified by latest permian neoendothyra in the zal section (Julfa area, NW Iran). *Rev. Esp. Micropaleontol.* 41, 197–213.

Altiner, D., Baud, A., Guex, J., and Stampfli, G. (1980). La limite permien-trias dans quelques localités du moyen-orient: recherches stratigraphiques et micropaléontologiques. *Riv. Ital. Paleontol. Stratigr.* 85, 683–714.

Atudorei, N. V. (1999). *Constraints on the Upper Permian to Upper Triassic Marine Carbon Isotope Curve. Case Studies from the Tethys*. PhD thesis. Switzerland: University of Lausanne, 160.

Baghbani, D. (1993). The permian sequence in the abadeh region, central Iran. *Occasional Publ. Earth Sci. Resour. Inst. Univ. S. C. New Ser. B* 9, 7–22.

Bando, Y. (1981). Discovery of lower triassic ammonites in the abadeh region of Central Iran. *Geol. Surv. Iran Rep.* 49, 73–103.

Baud, A. (1998). "Marine carbonate and siliceous factories: global change after the end of permian mass extinction," in *Proceedings of the 15th International Sedimentological Congress, Abstract Volume Alicante Spain* (Alicante: Universidad de Alicante), 180

Baud, A. (2018). Maurizio Gaetani, 1940-2017, in Memorandum. *Albertiana* 44, 60–64.

Baud, A., and Richoz, S. (2013). "The smithian (Early Triassic) red ammonoid limestone of Oman, refuge for sponge–microbial build-ups during a recovery phase," in *Paper Presented at the 2013 GSA Annual Meeting in Denver. GSA Abstracts with Programs*, Vol. 45, (Boulder, CO: Geological Society Of America), 883.

Baud, A., and Richoz, S. (2019). "The latest permian red ammonoid limestone and the basal triassic sponge-microbial buildups, time specific facies on the cimmerian margin of Central Iran and Armenia," in *Proceedings of the STRATI 2019*, (Roma: Società Geologica Italiana), 398.

Baud, A., Bucher, H., Brosse, M., Frisk, A., and Guodun, K. (2013). "Stromatactis limestone below and above the permian-triassic boundary event: evidence of sponge microbial build-up," in *World Summit on P-Tr Mass Extinction and Extreme Climate Change Abstract Book 8-9*, eds C. Zhong-Qiang, Y. Hao, and L. Genming (Wuhan: China University of Geosciences).

Baud, A., Cirilli, S., and Marcoux, J. (1997). Biotic response to mass extinction: the lowermost triassic microbialites. *Facies* 36, 238–242. doi: 10.1007/bf02536885

Baud, A., Friesenbichler, E., Krystyn, L., Sahakyan, L., and Richoz, S. (2015). "Proterozoic-like/type basal Triassic microbial build-ups of unusual height in Armenia," in *Proceedings of the Goldschmidt Conference, Prague August 16-21, 2015, Abstract book, 06i session, Poster 2074*, (Prague: Goldschmidt).

Baud, A., Richoz, S., and Pruss, S. (2007). The lower triassic anachronistic carbonate facies in space and time. *Glob. Planet. Change* 55, 81–89. doi: 10.1016/j.gloplacha.2006.06.008

Baud, A., Richoz, S., Cirilli, S., and Marcoux, J. (2002). "Basal Triassic carbonate of the Tethys: a microbialite world," in *Proceedings of the 16th International Sedimentological Congress, Johannesburg, RAU University, Abstract Vol. 24-25*, (Johannesburg: RAU University).

Besse, J., Torcq, F., Gallet, Y., Ricou, L. E., Krystyn, L., and Saidi, A. (1998). Late permian to late triassic palaeomagnetic data from iran: constraints on the migration of the iranian block through the tethyan ocean and initial destruction of Pangaea. *Geophys. J. Int.* 135, 77–92. doi: 10.1046/j.1365-246X.1998.00603.x

Brayard, A., Vennin, E., Olivier, N., Bylund, K. G., Jenks, J., Stephen, D. A., et al. (2011). Transient metazoan reefs in the aftermath of the end-Permian mass extinction. *Nat. Geosci.* 4, 693–697. doi: 10.1038/NGEO1264

Brunton, F. R., and Dixon, O. A. (1994). Siliceous sponge-microbe biotic associations and their recurrence through the Phanerozoic as reef mound constructors. *Palaios* 9, 370–387.

Chen, J., Shen, S. Z., Zhang, Y. C., Angiolini, L., Gorgij, M. N., Crippa, G., et al. (2020). Abrupt warming in the latest Permian detected using high-resolution in situ oxygen isotopes of conodont apatite from Abadeh, central Iran. *Palaeogeogr. Palaeoclimatol. Palaeoecol.* 560:109973. doi: 10.1016/j.palaeo.2020.109973

Corsetti, F. A., Baud, A., Marenco, J., and Richoz, S. (2005). Summary of early triassic carbon isotope records. *C. R. Palevol,* 4, 405–418. doi: 10.1016/j.crpv.2005.06.004

Corsetti, F. A., Ritterbush, K. A., Bottjer, D. J., Greene, S. E., Ibarra, Y., Yager, J. A., et al. (2015). Investigating the paleoecological consequences of supercontinent breakup: sponges clean up in the early Jurassic. *Sediment. Rec.* 13, 4–10. doi: 10.2110/sedred.2015.2

Coulson, K. P., and Brand, L. R. (2016). Lithistid sponge-microbial reef-building communities construct laminated, upper Cambrian (Furongian) 'stromatolites'. *Palaios* 31, 358–370. doi: 10.2110/palo.2016.029

Dudás, F. Ö, Yuan, D. X., Shen, S. Z., and Bowring, S. A. (2017). A conodont-based revision of the 87Sr/86Sr seawater curve across the Permian-Triassic boundary. *Palaeogeogr. Palaeoclimatol. Palaeoecol.* 470, 40–53. doi: 10.1016/j.palaeo.2017.01.007

Ezaki, Y., Liu, J., Nagano, T., and Adachi, N. (2008). Geobiological aspects of the earliest Triassic microbialites along the southern periphery of the tropical yangtze platform: initiation and cessation of a microbial regime. *Palaios* 23, 356–369. doi: 10.2110/palo.2007.p07-035r

Foster, W. J., Heindel, K., Richoz, S., Gliwa, J., Lehrmann, D. J., Baud, A., et al. (2019). Suppressed competitive exclusion enabled the proliferation of Permian/Triassic boundary microbialites. *Depos. Rec.* 2020, 62–74. doi: 10.1002/dep2.97

Friesenbichler, E. (2016). *Sedimentological Investigations on Lower Triassic Microbialites from Armenia*. Master Thesis at Institute of Earth Sciences. Graz: Graz University of Technology, 1–89.

Friesenbichler, E., Baud, A., Krystyn, L., Sahakyan, L., and Richoz, S. (2016). "Basal induan (Early Triassic) giant sponge-microbial build-ups in Armenia: microfacies analyses and carbon isotope studies," in *Paper Presented at the GSA Annual Meeting in Denver, Colorado, USA. Paper 225-11*, (Boulder, CO: Geological Society Of America).

Friesenbichler, E., Richoz, S., Baud, A., Krystyn, L., Sahakyan, L., Vardanyan, S., et al. (2018). Sponge-microbial buildups from the lowermost Triassic Chanakhchi section in southern Armenia: microfacies and stable carbon isotopes. *Palaeogeogr. Palaeoclimatol. Palaeoecol.* 490, 653–672. doi: 10.1016/j.palaeo.2017.11.056

Gaetani, M., Angiolini, L., Ueno, K., Nicora, A., Stephenson, M. H., Sciunnach, D., et al. (2009). Pennsylvanian–early triassic stratigraphy in the Alborz Mountains (Iran). *Geol. Soc. Lond. Spec. Publ.* 312, 79–128. doi: 10.1144/sp312.5

Gallet, Y., Krystyn, L., Besse, J., Saidi, A., and Ricou, L. E. (2000). New constraints on the Upper Permian and Lower Triassic geomagnetic polarity timescale from

the Abadeh section (central Iran). *J. Geophys. Res. Solid Earth* 105, 2805–2815. doi: 10.1029/1999jb900218

Gliwa, J., Ghaderi, A., Leda, L., Schobben, M., Tomás, S., Foster, W. J., et al. (2020). Aras valley (northwest Iran): high-resolution stratigraphy of a continuous central Tethyan Permian–Triassic boundary section. *Foss. Rec.* 23, 33–69. doi: 10.5194/fr-23-33-2020

Griffin, J. M., Marenco, P. J., Fraiser, M., and Clapham, M. E. (2010). "Stromatolite-sponge tubiphytes reefs in the virgin limestone member of the moenkopi formation, Nevada: implications for biotic recovery following the end-Permian mass extinction," in *Paper Presented at the Annual Meeting of the Geological Society of America Abstracts with Programs*, (Boulder, CO: Geological Society Of America), 72.

Grotzinger, J. P., and Knoll, A. H. (1995). Anomalous carbonate precipitates: is the precambrian the key to the permian? *Palaios* 10, 578–596.

Heindel, K., Foster, W. J., Richoz, S., Birgel, V. J., Roden, D., Baud, A., et al. (2018). The formation of microbial-metazoan bioherms and biostromes following the latest Permian mass extinction. *Gondwana Res.* 61, 187–202. doi: 10.1016/j.gr.2018.05.007

Heindel, K., Richoz, S., Birgel, D., Brandner, R., Klügel, A., Krystyn, L., et al. (2015). Biogeochemical formation of calyx-shaped carbonate crystal fans in the shallow subsurface of the Early Triassic seafloor. *Gondw. Res.* 27, 840–861. doi: 10.1016/j.gr.2013.11.004

Heuer, F., Leda, L., Korn, D., Hairapetian, V., and Moradi-Salimi, V. (2017). "Early Triassic microbialites at Baghuk (Central Iran)," in *Paper Presented at the Goldschmidt Conference, Paris August 13-18, 14d session Abstract book, 1621, Poster board 3142*, (Paris).

Heuer, F., Leda, L., Moradi-Salimi, V., Hairapetian, V., Gliwa, J., and Korn, D. (Submitted). The Permian-Triassic boundary section at Baghuk Mountain, Central Iran: carbonatemicrofacies and depositional environment. *Paleobiodivers. Paleoenviron. (Submitted).*

Heydari, E., and Hassanzadeh, J. (2003). Deev Jahi model of the permian-triassic boundary mass extinction: a case for gas hydrates as the main cause of biological crisis on Earth. *Sediment. Geol.* 163, 147–163. doi: 10.1016/j.sedgeo.2003.08.002

Heydari, E., Arzani, N., and Hassanzadeh, J. (2008). Mantle plume: the invisible serial killer — application to the permian–triassic boundary mass extinction. *Palaeogeogr. Palaeoclimatol. Palaeoecol.* 264, 147–162. doi: 10.1016/j.palaeo.2008.04.013

Heydari, E., Arzani, N., and Hassanzadeh, J. (2012). Elemental analysis of the uppermost Permian to the lowermost Triassic of the Shahreza section, Iran. *Abstr. Programs Geol. Soc. Am.* 62, 18–5.

Heydari, E., Arzani, N., Safaei, M., and Hassanzadeh, J. (2013). Ocean's response to a changing climate: clues from variations in carbonate mineralogy across the Permian–Triassic boundary of the Shahreza Section, Iran. *Glob. Planet. Change* 105, 79–90. doi: 10.1016/j.gloplacha.2012.12.013

Heydari, E., Hassandzadeh, J., and Wade, W. J. (2000). Geochemistry of central Tethyan upper permian and lower triassic strata, abadeh region, Iran. *Sediment. Geol.* 137, 85–99.

Heydari, E., Hassanzadeh, J., Wade, W. J., and Ghazi, A. M. (2003). Permian-Triassic boundary interval in the Abadeh section of Iran with implications for mass extinction: Part 1- Sedimentology. *Palaeogeogr. Palaeoclimatol. Palaeoecol.* 193, 405–423.

Heydari, E., Wade, W. J., and Hassanzadeh, J. (2001). Diagenetic origin of carbon and oxygen isotope compositions of Permian-Triassic boundary strata. *Sediment. Geol.* 143, 191–197. doi: 10.1016/S0037-0738(01)00095-1

Horacek, M., Brandner, R., and Abart, R. (2007a). Carbon isotope record of the P/T boundary and the Lower Triassic in the Southern Alps: evidence for rapid changes in storage of organic carbon. *Palaeogeogr. Palaeoclimatol. Palaeoecol.* 252, 347–354. doi: 10.1016/j.palaeo.2006.11.049

Horacek, M., Koike, T., and Richoz, S. (2009). Lower Triassic $\delta^{13}C$ isotope curve from shallow-marine carbonates in Japan, Panthalassa realm: confirmation of the Tethys $\delta^{13}C$ curve. *J. Asian Earth Sci.* 36, 481–490. doi: 10.1016/j.jseaes.2008.05.005

Horacek, M., Krystyn, L., and Baud, A. (2021). Comment to Chen et al., 2020: abrupt warming in the latest Permian detected using high-resolution in situ oxygen isotopes of conodont apatite from Abadeh, central Iran. Importance of correct stratigraphic correlation, reporting of existing data and their scientific interpretation. *Permophiles* 70, 33–36.

Horacek, M., Richoz, S., Brandner, R., Krystyn, L., and Spotl, C. (2007b). Evidence for recurrent changes in Lower Triassic oceanic circulation of the Tethys: the $\delta^{13}C$ record from marine sections in Iran. *Palaeogeogr. Palaeoclimatol. Palaeoecol.* 252, 355–369. doi: 10.1016/j.palaeo.2006.11.052

Horacek, M., Wang, X.-D., Grossman, E. L., Richoz, S., and Cao, C.-Q. (2007c). The carbon-isotope curve from the Chaohu section, China: different trends at the Induan-Olenekian Boundary or diagenesis? *Albertiana* 35:41–45.

Insalaco, E., Virgone, A., Courme, B., Gaillot, J., Kamali, M., Moallemi, A., et al. (2006). Upper dalan member and kangan formation between the zagros mountains and offshore fars, iran: depositional system, biostratigraphy and stratigraphic architecture. *Geoarabia* 11, 75–176.

Joachimski, M. M., Alekseev, A. S., Grigoryan, A., and Gatovsky, Y. A. (2020). Siberian Trap volcanism, global warming and the Permian-Triassic mass extinction: new insights from Armenian Permian-Triassic sections. *GSA Bull.* 132, 427–443. doi: 10.1130/B35108.1

Kershaw, S., Li, Y., Crasquin-Soleau, S., Feng, Q., Mu, X., Collin, P.-Y., et al. (2007). Earliest Triassic microbialites in the South China block and other areas: controls on their growth and distribution. *Facies* 53, 409–425. doi: 10.1007/s10347-007-0105-5

Kershaw, S., Zhang, T., and Lan, G. (1999). A? microbialite crust at the Permian-Triassic boundary in south China, and its palaeoenvironmental significance. *Palaeogeogr. Palaeoclimatol. Palaeoecol.* 146, 1–18.

Korte, C., and Kozur, H. W. (2010). Carbon-isotope stratigraphy across the permian-triassic boundary: a review. *J. Asian Earth Sci.* 39, 215–235. doi: 10.1016/j.jseaes.2010.01.005

Korte, C., Kozur, H., and Mohtat-Aghai, P. (2004a). Dzhulfian to lowermost Triassic δ13C record at the Permian/Triassic boundary section at Shahreza, Central Iran. *Hallesches Jahrb. Geowiss. Reihe B* 18, 73–78.

Korte, C., Kozur, H. W., Joachimski, M. M., Strauss, H., Veizer, J., and Schwark, L. (2004b). Carbone, sulfur, oxygen and strontium isotope records, organic geochemistry and biostratigraphy across the Permian/Triassic boundary in Abadeh, Iran. *Int. J. Earth Sci.* 9, 565–581. doi: 10.1007/s00531-004-0406-7

Korte, C., Pande, P., Kalia, P., Kozur, H. W., Joachimski, M. M., and Oberhänsli, H. (2010). Massive volcanism at the Permian–Triassic boundary and its impact on the isotopic composition of the ocean and atmosphere. *J. Asian Earth Sci.* 37, 293–311. doi: 10.1016/j.jseaes.2009.08.012

Kozur, H. (2004). Pelagic uppermost Permian and the Permian-Triassic boundary conodonts of Iran, Part 1: taxonomy. *Hallesches Jahrb. Geowiss. Reihe B* 18, 39–68.

Kozur, H. (2005). Pelagic uppermost permian and the permian-triassic boundary conodonts of Iran. Part II: investigated sections and evaluation of the conodont faunas. *Hallesches Jahrb. Geowiss. Reihe B* 19, 49–86.

Kozur, H. (2007). Biostratigraphy and event stratigraphy in Iran around the Permian-Triassic Boundary (PTB): implications for the causes of the PTB biotic crisis. *Glob. Planet. Change* 55, 155–176. doi: 10.1016/j.gloplacha.2006.06.011

Leda, L., Korn, D., Ghaderi, A., Hairapetian, V., Struck, U., and Reimold, W. U. (2014). Lithostratigraphy and carbonate microfacies across the Permian–Triassic boundary near Julfa (NW Iran) and in the Baghuk Mountains (Central Iran). *Facies* 60, 295–325. doi: 10.1007/s10347-013-0366-0

Lee, J.-H., and Hong, J. (2019). Sedimentologic and paleoecologic implications for keratose-like sponges in geologic records. *J. Geol. Soc. Korea* 55, 735–748. doi: 10.14770/jgsk.2019.55.6.735

Liu, X. C., Wang, W., Shen, S. Z., Gorgij, M. N., Ye, F. C., Zhang, Y. C., et al. (2013). Late Guadalupian to Lopingian (Permian) carbon and strontium isotopic chemostratigraphy in the Abadeh section, central Iran. *Gondwana Res.* 24, 222–232. doi: 10.1016/j.gr.2012.10.012

Luo, C. (2015). *Keratose" Sponge Fossils and Microbialites: A Geobiological Contribution to the Understanding of Metazoan Origin*. Ph.D thesis. Göttingen: Georg-August-Universität Göttingen, 151.

Luo, C., and Reitner, J. (2014). First report of fossil "keratose" demosponges in phanerozoic carbonates: preservation and 3-D reconstruction. *Naturwissenschaften* 101, 467–477.

Luo, C., and Reitner, J. (2016). 'Stromatolites' built by sponges and microbes - a new type of Phanerozoic bioconstruction. *Lethaia* 49, 555–570.

Luo, G., Algeo, T. J., Huang, J., Zhou, W., Wang, Y., Yang, H., et al. (2014). Vertical $\delta 13C_{org}$ gradients record changes in planktonic microbial community composition during the end-Permian mass extinction. *Palaeogeogr. Palaeoclimatol. Palaeoecol.* 396, 119–131. doi: 10.1016/j.palaeo.2014.01.006

Maaleki-Moghadam, M., Rafiei, B., Richoz, S., Woods, A. D., and Krystyn, L. (2019). Anachronistic facies and carbon isotopes during the end-Permian biocrisis: evidence from the mid-Tethys (Kisejin, Iran). *Palaeogeogr. Palaeoclimatol. Palaeoecol.* 516, 364–383. doi: 10.1016/j.palaeo.2018.12.007

Marenco, P. J., Griffin, J. M., Fraiser, M. L., and Clapham, M. E. (2012). Paleoecology and geochemistry of Early Triassic Spathian) microbial mounds and implications for anoxia following the end-Permian mass extinction. *Geology* 40, 715–718. doi: 10.1130/G32936.1

Mette, W. (2008). Upper Permian and lowermost Triassic stratigraphy, facies and ostracods in NW Iran. Implications for the P/T extinction event. *Stratigraphy* 5, 205–219.

Mohtat-Aghai, P., and Vachard, D. (2005). Late Permian foraminiferal assemblages from the Hambast Region (Central Iran) and their extinctions. *Revis. Esp. Micropaleontol.* 37, 205–227.

Mohtat-Aghai, P., and Vachard, D. (2003). Dagmarita shahrezahensis n. sp. globivalvulinid foraminifer (Wuchiapingian, late Permian, Central Iran). *Riv. Ital. Paleontol. Stratigr.* 109, 37–44. doi: 10.13130/2039-4942/5492

Payne, J. L., Lehrmann, D. J., Wei, J. Y., Orchard, M. J., and Knoll, A. H. (2004). Large perturbations of the carbon cycle during recovery from the end-Permian extinction. *Science* 305, 506–509.

Pruss, S. B., Bottjer, D. J., Corsetti, F. A., and Baud, A. (2006). A global marine sedimentary response to the end-Permian mass extinction: examples from southern Turkey and the western United States. *Earth Sci. Rev.* 78, 193–206. doi: 10.1016/j.earscirev.2006.05.002

Richoz, S. (2006). "Stratigraphie et variations isotopiques du carbone dans le Permien supérieur et le Trias inférieur de la Néotéthys (Turquie, Oman et Iran)," in *Mémoires de Géologie (Lausanne)*, Vol. 46, ed. J. Guex (Lausanne: Geological Museum), 1–264.

Richoz, S., Krystyn, L., Baud, A., Brandner, R., Horacek, M., and Mohtat-Aghai, P (2010). Permian-Triassic boundary interval in the Middle East (Iran and N. Oman): progressive environmental change from detailed carbonate carbon isotope marine curve and sedimentary evolution. *J. Asian Earth Sci.* 39, 236–253. doi: 10.1016/j.jseaes.2009.12.014

Riding, R. (2008). Abiogenic, microbial and hybrid authigenic carbonate crusts: components of Precambrian stromatolites. *Geol. Croat.* 61, 73–103.

Sahakyan, L., Baud, A., Grigoryan, A., Friesenbichler, E., and Richoz, S. (2017). "The permian-triassic transition in Southern Armenia," in *Proceeding of the 5th IGCP 630 International conference and field workshop, 8-14 10, 2017*, (Yerevan: National Academy of Sciences of the Armenia Republic), 1–53.

Schobben, M., Joachimski, M. M., Korn, D., Leda, L., and Korte, C. (2014). Palaeotethys seawater temperature rise and an intensified hydrological cycle following the end-Permian mass extinction. *Gondwana Res.* 26, 675–683. doi: 10.1016/j.gr.2013.07.019

Schobben, M., Stebbins, A., Ghaderi, A., Strauss, H., Korn, D., and Korte, C. (2015). Flourishing ocean drives the end-Permian marine mass extinction. *Proc. Natl. Acad. Sci. U.S.A.* 112, 10298–10303. doi: 10.1073/pnas.1503755112

Schobben, M., Ullmann, C. V., Leda, L., Korn, D., Struck, U., Reimold, W. U., et al. (2016). Discerning primary versus diagenetic signals in carbonate carbon and oxygen isotope records: an example from the Permian–Triassic boundary of Iran. *Chem. Geol.* 422, 94–107. doi: 10.1016/j.chemgeo.2015.12.013

Schobben, M., van de Velde, S., Gliwa, J., Leda, L., Korn, D., Struck, U., et al. (2017). Latest Permian carbonate carbon isotope variability traces heterogeneous organic carbon accumulation and authigenic carbonate formation. *Clim. Past* 13, 1635–1659.

Sedlacek, A. R., Saltzman, M. R., Algeo, T. J., Horacek, M., Brandner, R., Foland, K., et al. (2014). 87Sr/86Sr stratigraphy from the early triassic of Zal, Iran: linking temperature to weathering rates and the tempo of ecosystem recovery. *Geology* 429, 779–782. doi: 10.1130/G35545.1

Shapiro, R. S., and Awramik, S. M. (2006). Favosamaceriacooperi new group and form: A widely dispersed, time-restricted thrombolite. *J. Paleontol.* 80, 411–422. doi: 10.1666/0022-3360(2006)80[411:FCNGAF]2.0.CO;2

Shen, S. Z., and Mei, S. L. (2010). Lopingian (Late Permian) high-resolution conodont biostratigraphic in Iran with comparison to South China zonation. *Geol. J.* 45, 135–161. doi: 10.1002/gj.1231

Shen, S. Z., Cao, C. Q., Zhang, H., Bowring, S. A., Henderson, C. M., Payne, J. L., et al. (2013). High-resolution δ13Ccarb chemostratigraphy from latest Guadalupian through earliest Triassic in South China and Iran. *Earth Planet. Sci. Lett.* 375, 156–165. doi: 10.1016/j.epsl.2013.05.020

Stampfli, G. M., and Borel, G. D. (2002). A plate tectonic model for the Paleozoic and Mesozoic constrained by dynamic plate boundaries and restored synthetic oceanic isochrons. *Earth Planet. Sci. Lett.* 196, 17–33.

Szulc, J. (2003). "Sponge-microbial stromatolites and coral-sponge reefs recovery in the Triassic of Western Tethys and Northern Peri-Tethys basins," in *Proceedings of the 9th Intern. Symposia on Fossil Cnidaria and Porifera*, Vol. 7, (Graz: Institute für Geologie und Paläontologie), 108.

Szulc, J. (2007). Sponge-microbial stromatolites and coral-sponge reef recovery in the Triassic of the western Tethys domain. *N. M. Mus. Nat. Hist. Sci. Bull.* 41:402.

Szulc, J. (2010). "Early and middle triassic recovery of the carbonate biofactory in the Western Tethys domain," in *Proceedings of the Second IGCP 572 field workshop, Feb (20-26, 2010, in the Sultanate of Oman, Abstract book 9*, (Antalya: IGCP).

Taraz, H. (1969). Permo-Triassic section in central Iran. *Am. Assoc. Pet. Geol. Bull.* 533, 688–693.

Taraz, H. (1971). Uppermost permian and permo-triassic transition beds in Central Iran. *Am. Assoc. Pet. Geol. Bull.* 55, 1280–1294.

Taraz, H. (1973). Correlation of uppermost permian in Iran, Central-Asia, and South China. *Am. Assoc. Pet. Geol. Bull.* 57, 1117–1133.

Taraz, H. (1974). Geology of the surmaq – deh bid area, abadeh region, Central Iran. *Geol. Surv. Iran Rep.* 37, 1–148.

Taraz, H., Golshani, F., Nakazawa, K., Shimura, D., Bando, Y., Ishii, K.-I., et al. (1981). The permian and the lower triassic systems in abadeh region, Central Iran. *Mem. Fac. Sci. Kyoto Univ. Ser. Geol. Mineral.* 47, 62–133.

Vennin, E., Olivier, N., Brayard, A., Bour, I., Thomazo, C., Escarguel, G., et al. (2015). Microbial deposits in the aftermath of the end−Permian mass extinction: a diverging case from the Mineral Mountains (Utah, USA). *Sedimentology* 62, 753–792. doi: 10.1111/sed.12166

Wang, T., Burne, R. V., Yuan, A., Wang, Y., and Yi, Z. (2019). The evolution of microbialite forms during the Early Triassic transgression: a case study in Chongyang of Hubei Province, South China. *Palaeogeogr. Palaeoclimatol. Palaeoecol.* 519, 209–220. doi: 10.1016/j.palaeo.2018.01.043

Wang, W. Q., Garbelli, C., Zhang, F. F., Zheng, Q. F., Zhang, Y. C., Yuan, D. X., et al. (2020). A high-resolution Middle to Late Permian paleotemperature curve reconstructed using oxygen isotopes of well-preserved brachiopod shells. *Earth Planet. Sci. Lett.* 540:116245. doi: 10.1016/j.epsl.2020.116245

Wang, W., Kano, A., Okumura, T., Ma, Y., Matsumoto, R., Matsuda, N., et al. (2007). Isotopic chemostratigraphy of the microbialite-bearing Permian-Triassic boundary section in the Zagros Mountains, Iran. *Chem. Geol.* 244, 708–714. doi: 10.1016/j.chemgeo.2007.07.018

Wardlaw, B. R., and Davydov, V. I. (2005). Progress report of the permian–triassic time slice project. *Permophiles* 45, 36–39.

Wei, W., Matsumoto, R., Kakuwa, Y., Mahmudy Gharaie, M. H., Yue, L., Kano, A., et al. (2005). Isotopic chemostratigraphy of the permian–triassic boundary in zagros mountains, Aligoudarz, Iran. *Permophiles* 45, 31–36.

Wignall, P. B., and Twitchett, R. J. (2002). Extent, duration, and nature of the permian-triassic superanoxic event. *Spec. Pap. Geol. Soc. Am.* 395–414.

Wignall, P. B., Woods, A., and Bottjer, D. (2005). Comment on "Permian-Triassic boundary interval in the Abadeh section of Iran with implications for mass extinction: part 1. Sedimentology" by E. Heydari, J. Hassanzadeh, W.J. Wade and A.M. Ghazi, 2003. Palaeogeography Palaeoclimatology Palaeoecology 193, 405-424. *Palaeogeogr. Palaeoclimatol. Palaeoecol.* 217, 315–317. doi: 10.1016/j.palaeo.2004.11.022

Woods, A. D. (2014). Assessing Early Triassic paleoceanographic conditions via unusual sedimentary fabrics and features. *Earth Sci. Rev.* 137, 6–18. doi: 10.1016/j.earscirev.2013.08.015

Woods, A. D., and Baud, A. (2008). Anachronistic facies from a drowned Lower Triassic carbonate platform: lower member of the Alwa Formation (Ba'id Exotic), Oman Mountains. *Sediment. Geol.* 209, 1–14. doi: 10.1016/j.sedgeo.2008.06.002

Woods, A. D., Bottjer, D. J., and Corsetti, F. A. (2007). Calcium carbonate seafloor precipitates from the outer shelf to slope facies of the Lower Triassic (Smithian-Spathian) UnionWash Formation, California, U.S.A.: sedimentology and palaeobiologic significance. *Palaeogeogr. Palaeoclimatol. Palaeoecol.* 252, 281–290. doi: 10.1016/j.palaeo.2006.11.053

Woods, A. D., Bottjer, D. J., Mutti, M., and Morrison, J. (1999). Lower Triassic large sea-floorcarbonate cements: their origin and a mechanism for the prolonged biotic recoveryfrom the end-Permian mass extinction. *Geology* 27, 645–648.

Yang, H., Chen, Z. Q., Kershaw, S., Liao, W., Lü, E., and Huang, Y. (2019). Small microbialites from the basal Triassic mudstone (Tieshikou, Jiangxi, South China): geobiologic features, biogenicity, and paleoenvironmental implications. *Palaeogeogr. Palaeoclimatol. Palaeoecol.* 519, 221–235. doi: 10.1016/j.palaeo.2018.06.030

Zhang, F., Romaniello, S. J., Algeo, T. J., Lau, K. V., Clapham, M. E., Richoz, S., et al. (2018). Multiple episodes of extensive marine anoxia linked to global warming and continental weathering following the latest Permian mass extinction. *Sci. Adv.* 4:e1602921.

Zong-jie, F. (2005). Comment on "Permian-Triassic boundary interval in the Abadeh section of Iran with implications for mass extinction: part 1– : sedimentology" by E. Heydari, J. Hassanzadeh, W.J. Wade and A.M. Ghazi 2003. Palaeogeography Palaeoclimatology Palaeoecology 193:405-424. *Palaeogeogr. Palaeoclimatol. Palaeoecol.* 217, 311–314. doi: 10.1016/j.palaeo.2004.11.021

Conflict of Interest: The authors declare that the research was conducted in the absence of any commercial or financial relationships that could be construed as a potential conflict of interest.